ISSN 0736-5306

SCIENCE OF

TSUNAMI HAZARDS

The International Journal of The Tsunami Society

Volume 11 Number 2 1993

MODELING THE TSUNAMI FROM THE 1917
HALIFAX HARBOUR EXPLOSION 67
David A. Greenberg
Bedford Institute of Oceanography, Dartmouth, Canada
T. S. Murty
Institute of Ocean Sciences, Sidney, Canada
Alan Fuffman
Geomarine Associates Ltd., Halifax, Canada

NUMERICAL TSUNAMI SOURCE STUDY - II 81
Charles L. Mader, Dennis W. Moore
University of Hawaii, Honolulu, U.S.A.
George F. Carrier
Harvard University, Cambridge, U.S.A.

NUMERICAL TSUNAMI PROPAGATION STUDY - III 93
Charles L. Mader, Dennis W. Moore
University of Hawaii, Honolulu, U.S.A.
George F. Carrier
Harvard University, Cambridge, U.S.A.

MODELING THE 1992 NICARAGUA TSUNAMI 107
Charles L. Mader
University of Hawaii, Honolulu, U.S.A.

THREE DEADLY TSUNAMIS IN ONE YEAR 111
AUGUSTINE S. FURUMOTO
University of Hawaii, Honolulu, USA

SCENES OF DESTRUCTION FROM HOKKAIDO TSUNAMI 122
Dennis Sigrist
International Tsunami Information Center, Honolulu, USA

THE TSUNAMI RESEARCH PROBLEM 125
George D. Curtis
University of Hawaii, Honolulu, USA

OBJECTIVE: **The Tsunami Society** publishes this journal to increase and disseminate knowledge about tsunamis and their hazards.

DISCLAIMER: Although these articles have been technically reviewed by peers, **The Tsunami Society** is not responsible for the veractiy of any statement, opinion or consequences.

Submit manuscripts of articles, notes or letters to the Technical Editor. If an article is accepted for publication the author(s) must submit a camera ready manuscript in the journal format. A voluntary $50.00 page charge will include 50 reprints.

SUBSCRIPTION INFORMATION: Price per copy $20.00 USA

ISSN 0736-5306

Published by The Tsunami Society in Honolulu, Hawaii, USA

Modelling the Tsunami from the 1917 Halifax Harbour Explosion

DAVID A. GREENBERG

Physical and Chemical Sciences Branch, Department of Fisheries and Oceans, Bedford Institute of Oceanography, Dartmouth, N.S., CANADA

T. S. MURTY

Department of Fisheries and Oceans, Institute of Ocean Sciences, Sidney, B.C.,CANADA

ALAN RUFFMAN

Geomarine Associates Ltd., Halifax, N.S.,CANADA

Abstract.

With no functioning tide gauge and little quantitative record, it has in the past been difficult to put together a good picture of the tsunami that followed the explosion of the munition ship *Mont Blanc* in Halifax Harbour. We have used a finite element model initialized with a setup derived using the theory of explosions in water and the known quantity of explosive. The model results when put together with anecdotal reports give a consistent overview of the tsunami amplitude and progression. Our study indicates that in the Narrows at the explosion site, the wave was over 10m high, but that the amplitude diminished greatly further away. In the Bedford Basin the tsunami would not have been damaging and in the outer reaches of the harbour, it would have been noticeable only to those looking for it.

Introduction

In the midst of World War I, shortly before 9 a.m. on December 6, 1917 the munition ship Mont Blanc collided with the relief ship Imo in the Narrows of the Canadian port Halifax. The Mont Blanc was carrying the equivalent of about 2900 short tons (2000lb/ton) of TNT. A fire broke out on board the Mont Blanc and the crew abandoned ship. The ship drifted in to the Halifax side and grounded near one of the piers. Shortly after 9 a.m. the cargo exploded devastating a large section of the city. Estimates of the casualties are as high as 2000dead and 9000 injured. Of these, many are thought to have died from the effects of the tsunami that followed. The documented damage of this, the greatest man made explosion to that date, would later be used in the Manhattan project to estimate the devastation of the the first nuclear bombs [Simpson and Ruffman, 1993 in press].

There was not an operational tide gauge at the time recording the changes in sea level, but there are several narrative reports of extreme high and low water. We have examined many of these reports to see what quantitative information might be obtained from them ([Ruffman *et al.*, 1993 in press]). We do have available to us tide predictions and tidal constants based on observations from before and after the war years. These indicate that the tides then were not substantially different from the tides of today and that the explosion occurred very close to low tide, about 0.5m below mean water level. In this study, we will be referring to the water level displacement relative to the existing tide.

To hindcast the tsunami, we have run a linearized finite element model covering the full area of Halifax Harbour from the head of the Bedford Basin to the seaward entrance to the harbour approach. The model was initialized with a set up derived using an empirical formula for waves resulting from explosions in water. In another publication [Greenberg *et al.*, 1993] we look in detail at how we derive the initial set up and at the model results. In this paper we show how the amplitude of the tsunami correlates with some of the anecdotal information available to us.

The Numerical Model

The finite element mesh (Figure 1) covers the area from the head of Bedford Basin to the outer harbour entrance. The mesh was constructed to give good resolution around the explosion site in the narrows, and inner harbour with less detail in Bedford Basin and the outer reaches. The methodology and equations are described in [Werner and Lynch, 1987]. The linearized form of the wave and momentum equations as used in this study are:

$$\begin{aligned}\frac{\partial^2 H}{\partial t^2} &+ \tau_0 \frac{\partial H}{\partial t} - \nabla \cdot [gh\nabla\zeta \\ &+ \mathbf{f}\times h\mathbf{V} + (\tau - \tau_0)h\mathbf{V}] = 0\end{aligned} \quad (1)$$

$$\frac{\partial \mathbf{V}}{\partial t} + g\mathbf{V}\zeta + \mathbf{f}\times\mathbf{V} + \tau\mathbf{V} = 0 \quad (2)$$

Where:

h = depth of the undisturbed water

ζ = sea surface elevation

H = $h + \zeta$

g = acceleration due to gravity

$\mathbf{V}$ = (u, v) the (east,north) velocity

$\mathbf{f}$ = the Coriolis parameter

τ_0 = an arbitrary constant used to avoid drift in the numerical computations

τ = bottom stress, $= k/h$, $k = 0.001 m/s$

We use 1 to solve for ζ and equation 2 to solve for $\mathbf{V}$ at each time step. The model was run for 40 minutes with the water starting from rest and the elevation set up as described in the next section. To model the resultant wave from an initially imposed shock we need a time step much smaller than the usual numerical stability conditions would require. A time step of 0.25 seconds was used here.

The initial setup and boundary conditions

The computation of the initial water level displacement from a given amount of explosive in water is very much an inexact science. In reality, there would be a large depression created by the explosion and water would be pushed out in a concentric ring. Existing theory does not give the precise magnitude of the depression or the momentum of such a wave. Instead we rely on an empirical and experimental studies that give us a formula for the amplitude of the tsunami from an explosion at a given distance. A rearrangement of the formula given in [Van Dorn *et al.*, 1968] is:

$$\eta = \frac{\mathbf{A} \cdot y^{0.54}}{r} \tag{3}$$

Where η is the elevation in feet, $\mathbf{A}$ is an experimentally derived constant $\mathbf{A} = 10$ for deep explosions and $\mathbf{A} = 18$ for shallow explosions, y is the explosive force in pounds of TNT, and r is the distance from the center of the explosion in feet. In our study, we tested both $\mathbf{A} = 10$ and $\mathbf{A} = 18$. The value $\mathbf{A} = 18$ gave unreasonably high results when compared to the anecdotal evidence. The value $\mathbf{A} = 10$ was in good agreement with these records, but we can not assume that the explosion would meet the criteria for a deep wave. We do feel however that the energy input into the tsunami would have been reduced because the explosion took place in shallow water with one end of the ship actually grounded, thus energy that would have been transferred to the bottom was absorbed in the harbour floor. For our work we use the factor $\mathbf{A} = 10$ in 3 since the other approximations in the computation and the accuracy of our anecdotal data precludes any fine tuning of the results.

In a study of tsunamis [Murty, 1977] it was concluded that a stable propagating wave is limited in amplitude to 80% of the depth of the water in which it travels. In the Narrows by the explosion site, the maximum water depth is approximately 20m so we used 16m as the amplitude of the initial water level displacement. We initialize the model with the elevation field:

$$\begin{aligned}
\eta &= \eta_0 \cos(\frac{\pi}{6r}\sqrt{(x-x_0)^2+(y-y_0)^2}) \\
&\quad \sqrt{(x-x_0)^2+(y-y_0)^2} < 3r \\
&= 0 \\
&\quad \sqrt{(x-x_0)^2+(y-y_0)^2} > 3r
\end{aligned} \tag{4}$$

Where $\eta_0 = 16m$, (x_0, y_0) are the coordinates of the explosion site, and r is the radius, calculated using 3, and the explosive charge given above.

Along the coastal boundaries the normal velocity is set to zero and at the ocean boundary the elevation is set to zero for all time.

Model limitations

There are several aspects of the model which will limit the accuracy of our solutions. The linear friction, the absence of the advective terms and the ignoring of sea surface elevation with respect to the depth of water, will all contribute to an inaccurate time history of the tsunami [Murty, 1977]. The fixed elevation on the open boundary will feed an artificial negative reflection back into the model domain. The tides have been ignored in this computation. Since we are primarily interested in the maximum and minimum sea levels resulting from the explosion, we can still get useful information from this computation. Although the linearization will affect the form of the wave, we feel that the maximum and minimum amplitude of the tsunami will be approximately correct. It was found that the wave reaching the open boundary is small, and any reflection would also be small, and would have had an effect only on the later oscillations, not on the initial waves which gave rise to the maximum and minimum elevations. Halifax Harbour is essentially cotidal and the tidal range is small. The explosion occurred shortly after low tide which was approximately 0.5m below mean sea level. This value could be subtracted from the extrema computed here with the linear model, but given the other assumptions and the approximate solutions we are seeking, it was not thought useful to do so.

The time of arrival of the initial wave (Figure 2) is taken as the time the sea level first exceeded 0.2m. The first tsunami wave spreads from its initial specified area through the Narrows within 2 minutes, to the head of Bedford Basin and the mouth of the inner harbour within 8 minutes and to the model open boundary in 16-18 minutes. The plots of sea level through time at various locations (Figure 3) confirm that given this timing, there is minimal influence on the extreme values computed. The anecdotes collected in [Ruffman *et al.*, 1993 in press] are compared here to the model results shown here in figure 4. In the extremes of Bedford Basin and seaward of Georges Island the amplitude of the wave predicted in the model, is low and we have no reliable observational evidence for a tsunami in these areas. At the mouth of the Basin the ship the *Nieuw Amsterdam*, anchored in the Basin observed,

> At about 9.10 this morning the ship suffered two shocks, succeeding each other within a few seconds, the last more severe than the first. ... After the explosion a decided wave was observed over the bay, as the water was forced on by the expanding air.

In the harbour away from the Narrows, the reports of the tsunami from passengers on the Halifax-Dartmouth ferry are somewhat contradictory, but are qualitatively consistent with the 2-4m magnitude predicted in the model. There are two accounts from Dorothy Chisholm who stated:

> She remembers nothing of the tidal wave, of which others spoke... and later added:

> The tidal wave was more in the North End, and we didn't feel it.

Other passengers did notice the wave:

> Miss O'Regan has the impression that the ferry stopped completely for a moment and then started up again. Mrs. Johns said that she felt it sink down as if the harbour's waters had parted in the tidal wave, and then bob up again.

At the downtown waterfront, a ready comparison to the fixed piers was possible. The model's 2-4m predicted water level is consistent with the following account:

> Lucy Ann Slaunwhite's father and three or four others from Terrance Bay, N.S. were in Halifax the morning of December 6, 1917 moored in a boat on the downtown waterfront. Terrance Bay is about 20 km outside of Halifax on the Atlantic coast and it was not well-served by roads in 1917; it was common for local families to go by boat to Halifax for supplies. After the Explosion, "the tide lifted the boat right up over the wharf to which they were tied."

Within the Narrows the reports indicate a much higher water level: On the Dartmouth side of the harbour opposite the explosion site the model indicates there was a local maximum in elevation which is consistent with this account:

> At the time fire broke out on the steamer he [Phillip Mitchell] was on the Dartmouth shore ... opposite the steamers. Near him was an electric wire pole... When the explosion came ... [he] ran to the wire post... . Then, he says, came a huge wave, and he wrapped his arms about the post and held on. The water went away over his head and as it receded, he saw a box car on the track above him soaked with water as if the wave had covered it. That wave receded and then came another which only reached his arm pits and receded.

The computation also shows extremely high maximum and low minimum in the Tufts Cove area. Even though the minimum is not realistic because this area would have been dry at the levels (of withdrawal) indicated, the reports confirm the general magnitude:

> The tidal wave crashed against the Dartmouth side with incredible force. Tufts Cove, on the eastern shore of the Narrows, felt the full impact of the wave: the single-story houses there were swamped.

> Several families of Micmac Indians lived near the cove. Their homes were wrecked, and at least nine people were killed. George Dixon was working at a small shipbuilding plant in the cove. He said that the water was literally boiling with flying pieces of metal. When he and his brother-in-law got to their feet after the explosion, his brother-in-law said, "We might as well have been killed as to find this thing coming at us." [i.e. the 'tidal wave'].

Close to the explosion site, the anecdotal information confirms that the tsunami was severe. There are several reports that are similar to these:

> All of a sudden this big explosion come – and the next thing we knew when we come to, this big tidal wave swept right over the house. ... Our home was located on – right where the Texalocan[sic] tanks are on Barrington Street now. And that is – and then our backyard – You went down our backyard and went right over the tracks. And the ship was just to the right of the tracks.

> The tidal wave was one of the most curious phenomena of the explosion and has been almost overlooked in the record of the disaster. Survivors of the explosion say that the crest of the advancing wave swept across Campbell road, more than twenty feet above the level of the harbor, caught some firemen as high up as the armpits and carried them back across the hill to a watery grave. Tugs, it is reported, touched the bottom of the harbor in the recoil. One small steamer was blown clear over No. 6 pier.

> After the explosion then there came these three tidal waves. And it emptied Halifax Harbour right out. I remember looking at Halifax Harbour just a little stream of water down the middle like on the bottom there. There was everything, china cups and knives and forks and everything just dropped overboard. And that, that first wave – I guess it rose the ship above the dock. And when it went out and when she came down, she just snapped them lines like strings...

The model results do not indicate that the full width of the harbour would have been emptied, but do predict levels that would expose shallow areas near the shore. Given the imprecise nature of these reports, we are gratified to find that there is such agreement with the model.

Concluding Remarks

We have used a simplified model initialized with a very approximate initial water level displacement, and compared the results to some very old subjective anecdotal observations. We believe that even with these severe limitations we have put together for the first time a reasonable picture of the tsunami from the 1917 explosion in Halifax Harbour. Further anecdotal evidence has been assembled in [Ruffman *et al.*, 1993 in press]. We look in more detail at the initial set up used and the model results in [Greenberg *et al.*, 1993]. Further work is planned using a fully nonlinear model of the narrows area incorporating drying shoals and flooding coastal areas to see what further insights might be gained.

Acknowledgments.

We thank Gordon Fader of the Atlantic Geoscience Centre, Bedford Institute of Oceanography for suggesting this study and Dan Lynch Dartmouth College, Hanover NH, for useful discussion on aspects of the modelling. We made extensive use of the TRIGRID finite element grid generation and analysis package being developed by R.F. Henry, Institute of Ocean Sciences and R. Walters, United States Geological Service, Tacoma WA.

References

GREENBERG, D. A., MURTY, T. S., AND RUFFMAN, A. (1993). A Numerical Model for the Tsunami in Halifax Harbour due to the Explosion in December 1917. *Marine Geodesy*, 16:153–167.

MURTY, T. S. (1977). *Seismic Sea Waves - Tsunamis*. Supply and Services Canada, Ottawa Canada.

RUFFMAN, A., GREENBERG, D. A., AND MURTY, T. S. (1993 in press). The Tsunami from the 1917 explosion in Halifax Harbour. In HOWELL, C. AND RUFFMAN, A., editors, *Proceedings of the 1917 Explosion Conference, Halifax Dec 3-6 1992*. Nimbus Publishing /Gorsebrook Research Institute, Halifax Nova Scotia.

SIMPSON, D. W. AND RUFFMAN, A. (1993 in press). Explosions, Bombs and Bumps - Scientific Aspects of the 1917 Explosion in Halifax Harbour. In HOWELL, C. AND RUFFMAN, A., editors, *Proceedings of the 1917 Explosion Conference, Halifax Dec 3-6 1992*. Nimbus Publishing / Gorsebrook Research Institute, Halifax, Nova Scotia.

VAN DORN, W. G., LEMEHAUTE, B., AND HWANG, L. S. (1968). *Handbook of explosion generated water waves, Vol 1, State of the Art*. Number TC-130. Tetratech Inc., Pasadena California.

WERNER, F. E. AND LYNCH, D. R. (1987). Field verification of Wave Equation tidal dynamics in the English Channel and southern North Sea. *Advances in Water Resources*, 10:115–130.

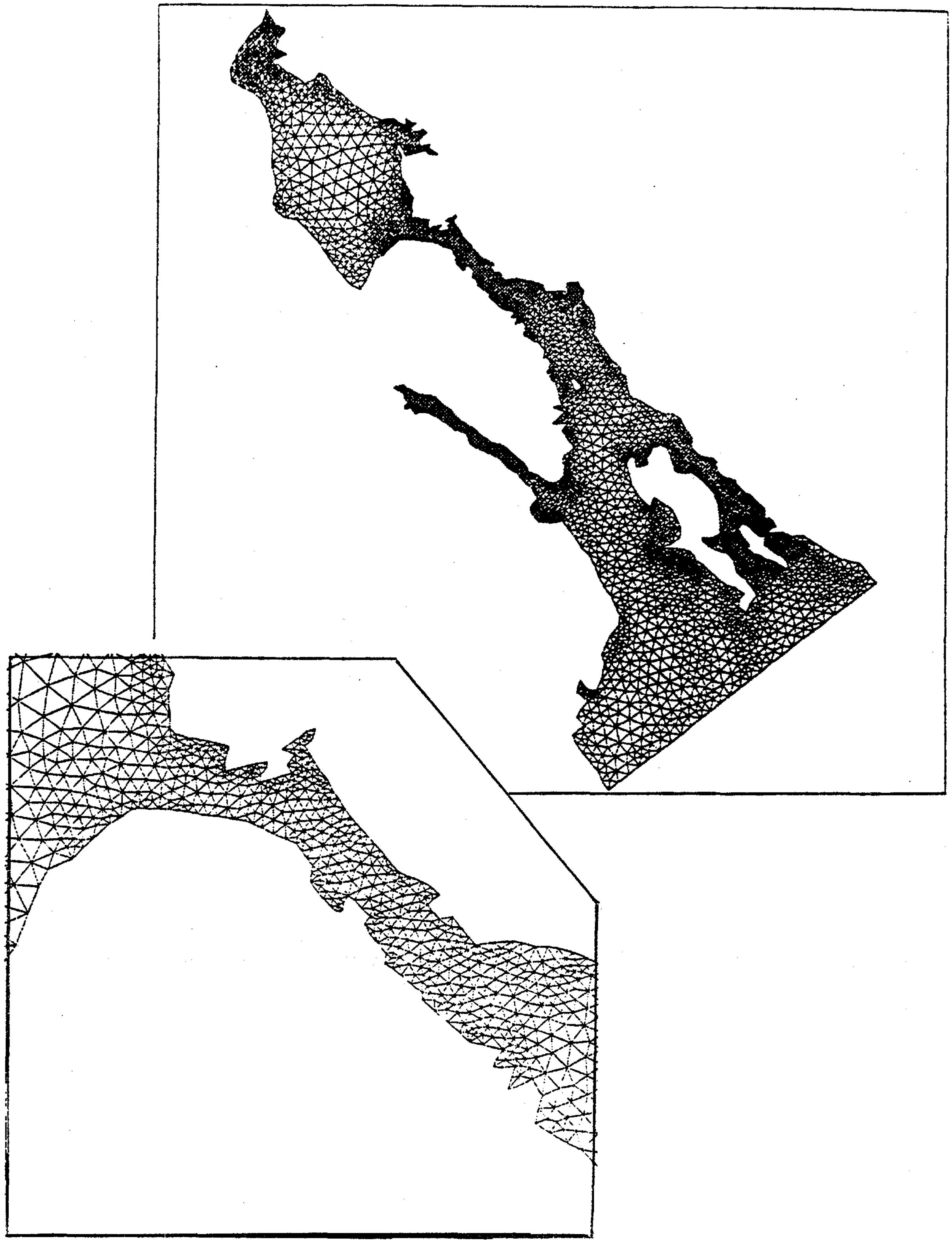

Figure 1: The finite element model mesh. The detail of the Narrows is shown in the lower left.

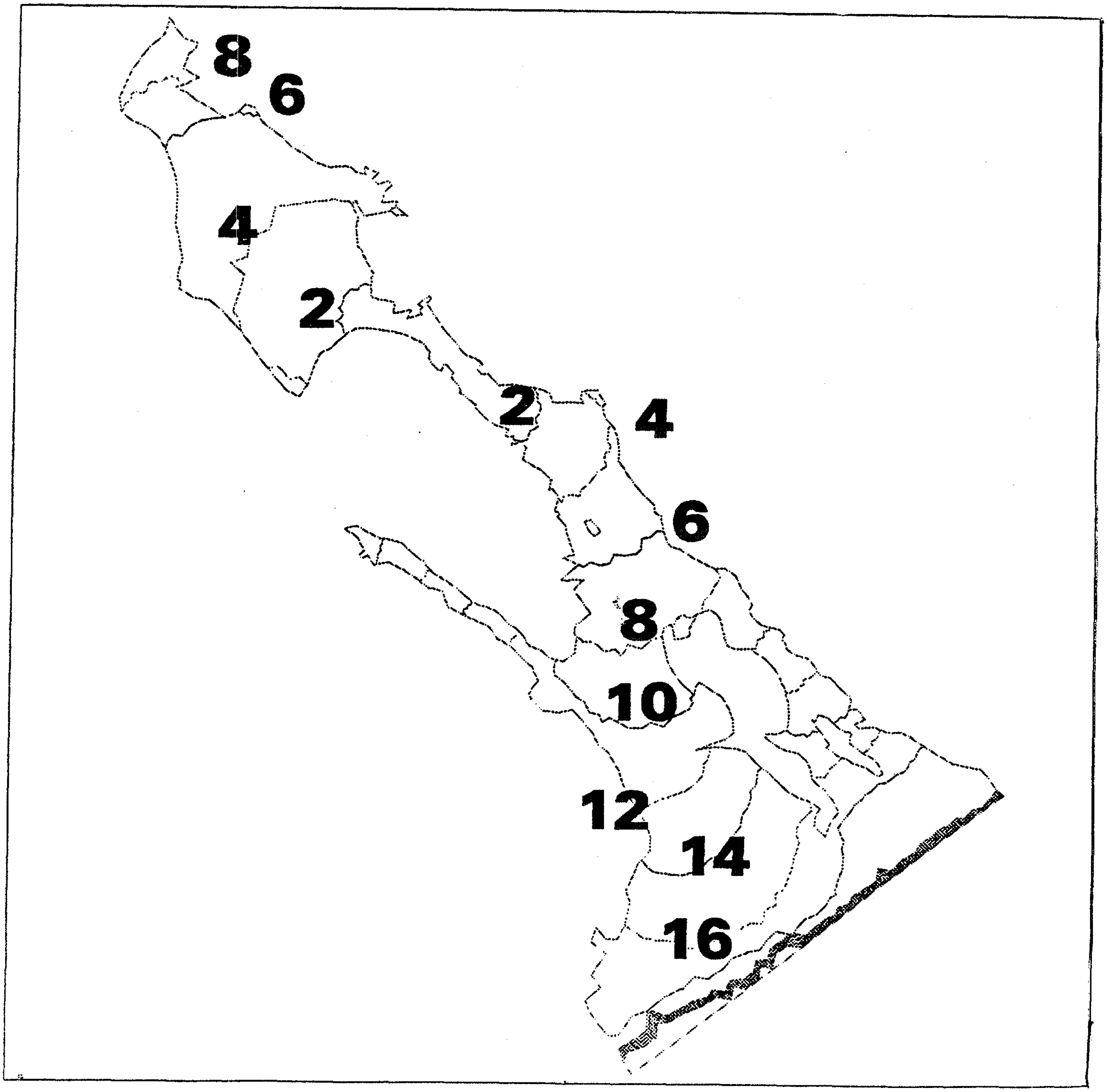

Figure 2: The time of arrival in minutes of the initial wave taken to be the time the sea level first exceeded $0.2m$.

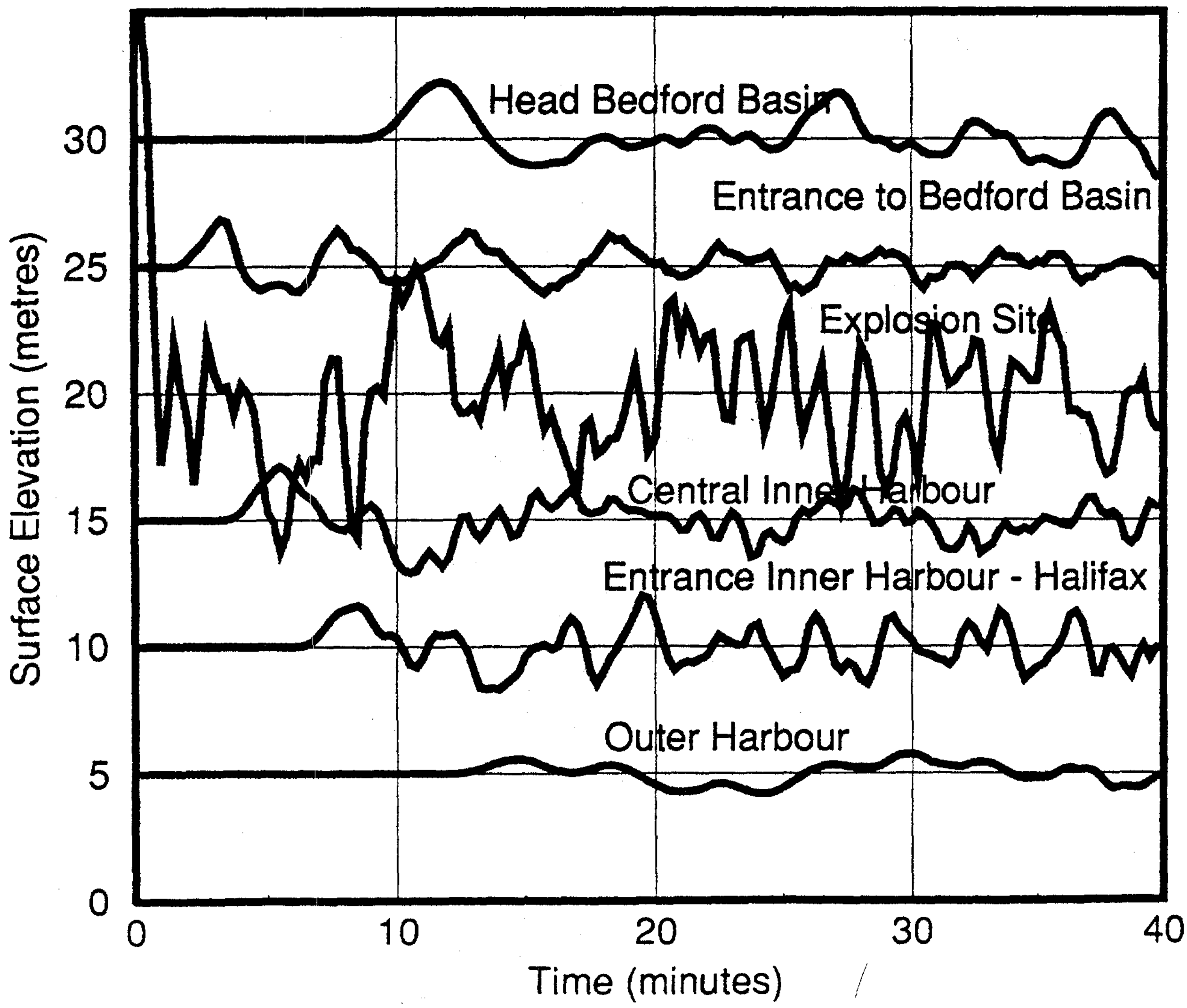

Figure 3: Time history of sea level at various locations. The curves are offset by $5m$.

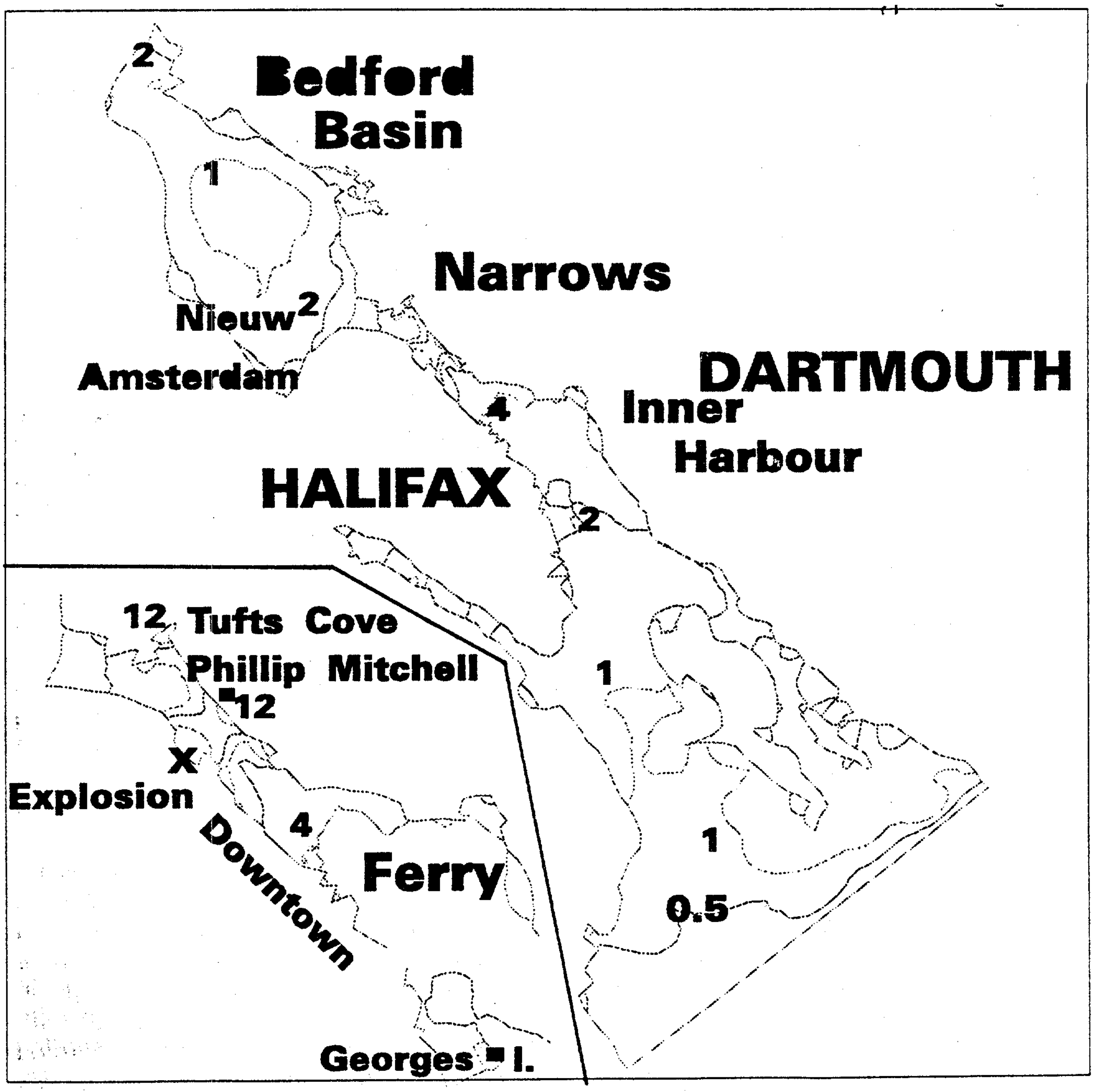

Figure 4: The maximum elevation achieved during the model run and locations (estimated) of the anecdotal observations. The detail of the Narrows is shown in the lower left.

NUMERICAL TSUNAMI SOURCE STUDY - II

Charles L. Mader
Dennis W. Moore
JTRE - JIMAR Joint Tsunami Research Effort
University of Hawaii, Honolulu, HI., U.S.A.
George F. Carrier
Harvard University, Cambridge, MA., U.S.A.

ABSTRACT

The *SWAN* code solves the nonlinear, shallow water, long wave equations including the effects of friction and flooding. Both the *SWAN* and *ZUNI* code which solves the incompressible Navier-Stokes equations were used to study the development of a tsunami wave from an initial sea surface displacement. The development of a tsunami wave was also modeled using two-dimensional linear gravity wave theory.

If the initial displacement is approximately Gaussian and the wavelength is very long compared to the depth, similar tsunami waves formed for all three methods. Two tsunami waves traveling in opposite directions formed that were the sum of the original surface displacement. However dispersion effects resulted in Navier-Stokes and linear gravity waves with decreasing front slopes, amplitudes, and by a train of small waves.

The shallow water wave has a constant vertical velocity while the Navier-Stokes and linear gravity waves have the more realistic variable vertical velocity. For long wave length tsunamis the constant vertical velocity closely reproduces the velocity characteristics of Navier-Stokes and linear gravity waves which slowly decrease with depth.

With decreasing periods and wavelengths, the discrepancy between the shallow water and the Navier-Stokes and linear gravity waves formed from initial sea surface displacement increases. This discrepancy as a function of the size of the tsunami source relative to the depth is characterized.

Introduction

The magnitude of the tsunami hazard at any land site depends upon the expected extent of flooding of the land by tsunamis at the site, the expected water velocities and the exposure of persons and property within the potential flood zone. The development of numerical models to describe tsunami wave generation, propagation and interaction with complicated topography such as bays or harbors and the resulting flooding has advanced to the stage where they are useful tools for determining the tsunami hazard in local regions. A numerical study of the flooding of Hilo, Hawaii by the tsunamis of April 1, 1946, May 23, 1960 and March 28, 1964 was described in reference 1.

The relative importance of the characteristics of the tsunami and the topography in and between the available models is being determined. The characterization of the tsunami flooding problem is a large and continuing effort. In this paper we describe the second study in our parameteric study of numerical and analytical tsunami models. The first study was described in reference 2. The effect of tsunami wave period, amplitude, bottom slope angle and friction on tsunami shoaling and flooding was investigated using a shallow water and a Navier-Stokes numerical model. The study showed higher wave shoaling and flooding for waves interacting with steeper slopes, for waves with longer periods and for waves from deeper water. The shallow water waves shoal higher, steeper and faster than the Navier-Stokes waves. The differences increase as the periods become shorter and slopes less steep with large differences for periods less than 500 seconds and slopes less than 2 percent.

The most common model used to describe tsunami generation, propagation and flooding is the nonlinear, shallow water, long wave model. A severe limitation to such models is called the "long wave paradox". The long wave model results in waves that become steeper as they move down a flat channel, that are too steep and move too fast as they shoal and therefore break too early. The problem is more serious as the distance and time of interest increases. Although the "long wave paradox" is a limitation on the accuracy of the results, the model can be very useful and inexpensive if applied cautiously to appropriate problems. Only recently have flooding capabilities been developed in the numerical models using the shallow water approximation, and we are continuing to make comparisions with more realistic models.

A more realistic description of water waves and flooding uses the Navier-Stokes equations. An early study of the shoaling and flooding using the Navier-Stokes equations is described in reference 3. In reference 2 we extended that study to examine the various parameters in more detail and in particular to compare with shallow water flooding results. In this study we examine the generation of a tsunami from an initial sea surface displacement as described using the Navier-Stokes equations. A study of the generation of water waves from cavities in the water surface and comparision with experimental observations is described in references 4, 5 and 6. The experimentally observed waves from cavities formed near the water surface were better reproduced by models using the Navier-Stokes equations than by models using the nonlinear shallow water equations. Explosively generated observed waves were deep water waves. Also described in reference 5 are the results of a study of the tsunami wave formed from an undersea landslide using the shallow water and the three-dimensional Navier-Stokes models. It was concluded that the shallow water model was not appropriate for studying waves generated from surface deformations that are small, relative to the water depth and that the nature of the surface collapse is different with the collapse occurring throughout the source region in the

Navier-Stokes calculations and mostly at the sides in the shallow water calculations.

In this study we examine the formation of a tsunami wave from an initial sea surface displacement similar to those obtained from earthquakes that have generated tsunami waves. Given an initial sea surface displacement, the characteristics of the tsunami wave formed using the non-linear shallow water model, the incompressible Navier-Stokes model, and the analytical linear gravity wave model are compared.

The Shallow Water Numerical Model

The *SWAN* code solves the incompressible, shallow water, long wave equations. It is described in detail in the monograph *Numerical Modeling of Water Waves* [4].

The incompressible, shallow water, long wave equations solved by the *SWAN* code are

$$\frac{\partial U_x}{\partial t} + U_x\frac{\partial U_x}{\partial x} + U_y\frac{\partial U_x}{\partial y} + g\frac{\partial H}{\partial x} = FU_y + F^{(x)} - g\frac{U_x(U_x^2+U_y^2)^{1/2}}{C^2(D+H-R)},$$

$$\frac{\partial U_y}{\partial t} + U_x\frac{\partial U_y}{\partial x} + U_y\frac{\partial U_y}{\partial y} + g\frac{\partial H}{\partial y} = -FU_x + F^{(y)} - g\frac{U_y(U_x^2+U_y^2)^{1/2}}{C^2(D+H-R)},$$

$$\frac{\partial H}{\partial t} + \frac{\partial(D+H-R)U_x}{\partial x} + \frac{\partial(D+H-R)U_y}{\partial y} - \frac{\partial R}{\partial t} = 0,$$

where U_x is velocity in x direction, U_y is velocity in y direction, g is gravitational acceleration, t is time, H is wave height above mean water level, R is bottom motion, F is Coriolis parameter, C is coefficient of DeChezy for bottom friction, $F^{(x)}, F^{(y)}$ are forcing functions of wind stress in x and y direction, and D is depth.

Flooding is described using positive values for depths below normal water level and negative values for elevations above normal water level. Only positive values of the $(D+H)$ terms in the above equations are permitted. This method results in both flooding and receeding surfaces being described by the *SWAN* code.

The *SWAN* code was used to model the effects of tides on the Musi-Upang estuaries, South Sumatra, Indonesia, by Safwan Hadi.[7] The *SWAN* code was used to model the large waves that were observed to occur inside Waianae harbor under high surf conditions in reference 8. The effect of the shape of a harbor cut through a reef on mitigating waves from the deep ocean was studied using the *SWAN* code in reference 9. Other examples of applications of the *SWAN* code are presented in reference 10. They include the wave motion resulting from tsunami waves interacting with a circular and triangular island surrounded by a 1/15 continental slope and from surface deformations in the ocean surface near the island. The effects of a surface deformation in the Sea of Japan similar to that of the May 1983 tsunami was modeled. The *SWAN* code was used to model the effect of wind and tsunami waves on Maunalua Bay, Oahu as described in reference 11. The interaction of a tsunami wave with a site of well documented topography on the South Kohala Coast of the Island of Hawaii was described in reference 12. The tsunami wave was calculated to flood the land to the 3 meter level and inundate the land between 90 and 120 meters from the shoreline.

The Navier-Stokes Numerical Model

The two-dimensional time dependent Navier-Stokes equations for incompressible flow solved by the *ZUNI* code are

$$\frac{\partial U_x}{\partial x} + \frac{\partial U_y}{\partial y} = 0 ,$$

$$\frac{\partial U_x}{\partial t} + U_x\left(\frac{\partial U_x}{\partial x}\right) + U_y\left(\frac{\partial U_x}{\partial y}\right) = -\frac{1}{\rho_o}\frac{\partial P}{\partial x} + g_x + \frac{\mu}{\rho_o}\left(\frac{\partial^2 U_x}{\partial x^2} + \frac{\partial^2 U_x}{\partial x \partial y}\right) ,$$

$$\frac{\partial U_y}{\partial t} + U_x\left(\frac{\partial U_y}{\partial x}\right) + U_y\left(\frac{\partial U_y}{\partial y}\right) = -\frac{1}{\rho_o}\frac{\partial P}{\partial y} + g_y + \frac{\mu}{\rho_o}\left(\frac{\partial^2 U_y}{\partial y \partial x} + \frac{\partial^2 U_y}{\partial y^2}\right)$$

where P is pressure and μ is the viscosity coefficient. A partial cell treatment that allows a rigid free slip obstacle to be placed through cell diagonals is included. The desired boundary slope is obtained by choosing the appropriate aspect ratio for the cells of the mesh. Thus, the numerical technique can be used to calculate wave run-up on exposed beaches in addition to submerged beaches. The details of the calculational procedure are described in reference 4.

The detailed Navier-Stokes numerical simulation of gravity waves that resemble the profile of actual tsunami waves was first achieved in reference 3. The interaction of tsunami waves with slopes that resembled the continental slope and shelf was simulated. Wave heights were calculated to increase by a factor of 4 as they shoaled up a 6.66 percent continental slope.

The *ZUNI* code was used to model the effect of submerged barriers on waves as described in references 3 and 4. The calculated transmission coefficients (ratio of wave height inside to height outside barrier) from experimental underwater barrier data were reproduced by the numerical model. Underwater barriers reflect significant amounts of the tsunami energy approaching a bay or harbor.

Water waves generated by explosions which produce bubbles underwater and cavities in the water surface have been described using the *ZUNI* code in references 4 and 5. The experimentally observed waves generated by cavities from explosions were deep water waves which were reproduced using the *ZUNI* code but not by the *SWAN* code.

The interaction of waves with submerged barriers and explosively generated water waves can not be described using the shallow water model since significant features of the flow are characteristic of deep water waves.

The Linear Gravity Wave Model

The analytical methods for solving the linear gravity wave model are described by Carrier in references 13 and 14. The two-dimensional linear gravity wave with a Gaussian, a square wave or a time dependent Gaussian displacement is solved using Fourier transforms by the *LGW* code for any time of interest. The wave description is obtained for any uniform depth, density, gravity and Gaussian break width or square wave half width. The wave height, vertical and horizontal velocities, and pressure are calculated at any depths desired. The distance scale is chosen to be a tenth of the Gaussian break width so that a wave half-width is described by about 50 space increments. Since the model is symmetrical about the center of the initial displacement, only half of the wave profile is calculated.

Initial Surface Displacement Study - *SWAN* Model

A 1 meter high Airy half wave surface displacement with a width of 45 kilometers in 4550 meter deep water was studied. This approximates within cell resolution a Gaussian wave with a Gaussian break width of 10 kilometers. The calculations were performed on an IBM PS/2 Model 95 computer using a version of the *SWAN* code that includes flooding and MCGRAPH graphics for the OS/2 operating system. Calculations were performed using a 250 meter wide mesh of 400 by 4 cells and at 0.5 second intervals.

The wave height in meters as a function distance is shown in Figure 1 at various times. The initial surface displacement separates into two shallow water waves with a height of 0.5 meter and length of 45 kilometers. At maximum height the vertical velocity at the center of the wave is 0.0232 meters/sec. An Airy wave with a 0.5 meter half width, 90 km wavelength in 4450 meters of water has a vertical velocity of 0.0235 to 0.0226 meters/sec at maximum height. The wave speed is 208.36 and the group velocity is 202.89 meters/s. The shallow water approximation used in the *SWAN* code of constant vertical velocity introduces errors of about 5 percent.

The non-linear feature of the shallow water model included in the *SWAN* code results in a small trailing wave with an amplitude of less than 0.01 meter.

Initial Surface Displacement Study - *ZUNI* Model

A 1 meter high approximately (within cell resolution) Gaussian surface water displacement with Gaussian break width of 10 km (which is equivalent to an Airy wave with a half-wavelength of 45 kilometers) in 4550 meter deep water was studied. The calculations for this geometry were performed with 15 cells in the *Y* or depth direction and 68 cells in the *X* or distance direction. The cells were rectangles 450 meters high in the *Y* direction and 4000 meters long in the *X* direction. The time increment was 3 seconds. The water level was placed at 4550 meters or 50 meters up into the eleventh cell. The viscosity coefficient used was 0.02 poise, a value representative of the actual viscosity for water. The viscosity did not significantly affect the results.

These results are an extension of those described in references 2, 3 and 4. The calculations were performed on an IBM PS/2 Model 95 computer using a special version of the *ZUNI* code that includes flooding and MCGRAPH graphics for the OS/2 operating system.

The wave height in meters as a function of distance is shown in Figure 2 at various times. The initial surface displacement separates into two nearly shallow water waves with a height of 0.5 meter and length of 45 kilometers. At 100 seconds the two waves have formed and the vertical velocity at the center of the wave is 0.0231 meters/sec at the top of the wave to 0.2158 meters/sec near the bottom of the wave. An Airy wave with a 0.5 meter half width, 90 km wavelength in 4450 meters of water has a vertical velocity of 0.0235 to 0.0226 meters/sec at the center of the wave. The Airy wave speed is 208.36 and the group velocity is 202.89 meters/s.

As the wave propagates the wave height decreases, the slope of the front of the wave becomes less, and small waves form behind the main wave. After the wave has propagated for 500 seconds, the wave height has decreased to 0.445 meters, and the vertical velocity at the center of the wave has decreased to 0.0217 meters/s near the peak of the wave to 0.0203 at the bottom of the wave. A train of waves has developed behind the main waves with maximum negative amplitude of 0.1 meter and positive amplitude of 0.05 meter.

Initial Surface Displacement Width Study - *LGW* Model

The linear gravity wave model was used to investigate the waves formed from initial surface displacements of width to depth ratios of 40 to 0.5 (Gaussian break widths of 40 to .5 kilometers) in 4550 meters deep water. The wave height after the wave had travel ten times its initial width for depth ratios of 40, 20, 10, 5, 1, 0.5 are shown in Figure 4.

The use of non-linear shallow water models to describe tsunami waves generated from earthquake generated surface displacements is adequate for tsunamis generated by surface displacements that are at least ten times wider than the depth. The non-linear shallow water wave becomes less realistic the further it travels from its source and the smaller the width to depth ratio. Non-linear shallow water models are adequate for large wave length and long period tsunamis such as generated by the 1964 Alaskan or the 1960 Chile earthquakes where the periods were about 30 minutes and wavelength to depth ratio in the deep ocean was greater than 80. Tsunami waves generated by earthquakes with small areas and periods of a few minutes will not be realistically described using shallow water models. Either the linear gravity wave model or better the Navier-Stokes model should be used for accurate modeling of tsunamis with small (less than 10) width to depth ratios.

Conclusions

The *SWAN* code solves the nonlinear, shallow water, long wave equations including the effects of friction and flooding. Both the *SWAN* and *ZUNI* code which solves the incompressible Navier-Stokes equations were used to study the development of a tsunami wave from an initial sea surface displacement. The development of a tsunami wave was also modeled using two-dimensional linear gravity wave theory.

If the initial displacement is approximately Gaussian and the wavelength is very long compared to the depth, similar tsunami waves formed for all three methods. Two tsunami waves traveling in opposite directions formed that were the sum of the original surface displacement. However dispersion effects resulted in Navier-Stokes and linear gravity waves with decreasing front slopes, amplitudes, and followed by a train of small waves.

The shallow water wave has a constant vertical velocity while the Navier-Stokes and linear gravity waves have the more realistic variable vertical velocity. For long wave length tsunamis the constant vertical velocity closely reproduces the velocity characteristics of Navier-Stokes and linear gravity waves which slowly decrease with depth.

With decreasing periods and wavelengths, the discrepancy between the shallow water and the Navier-Stokes and linear gravity waves formed from initial sea surface displacement increases.

Only part of the parameteric region of interest for tsunami generation, propagation and flooding has been investigated, particularly for the Navier-Stokes model. Since three-dimensional Navier-Stokes solutions to tsunami problems currently have limited practical application, most tsunami flooding studies will need to be performed using the shallow water model. These studies permit us to determine the parameteric region where the shallow water model can be useful.

Acknowledgments

The author gratefully acknowledges the contributions of G. D. Curtis, and H. G. Loomis of the University of Hawaii, Z. Kowalik of the University of Alaska, T. S. Murty of the Institute of Ocean Sciences, and E. N. Bernard of the Pacific Marine Environmental Laboratory.

References

1. Charles L. Mader and George D. Curtis, "Modeling Hilo, Hawaii Tsunami Inundation," Science of Tsunami Hazards, Vol 9, 85-94 (1991).
2. Charles L. Mader, "Numerical Tsunami Flooding Study - I ," Science of Tsunami Hazards, Vol 8, 79-96 (1990).
3. Charles L. Mader, "Numerical Simulation of Tsunamis," Journal of Physical Oceanography, Vol. 5, pp. 75–82 (1975).
4. Charles L. Mader *Numerical Modeling of Water Waves,* University of California Press, Berkeley, California (1988).
5. Charles L. Mader, Robert E. Tangora, and B. D. Nichols, "A Model of the 1975 Hawaii Tsunami," Natural Science of Hazards Vol 1, C1-8 (1982).
6. Charles L. Mader, "A Landslide Model for the 1975 Hawaii Tsunami," Science of Tsunami Hazards, Vol 2, 71-78 (1984).
7. Safwan Hadi, "A Numerical Tidal Model of Musi-Upang Estuaries." A dissertation submitted to Oceanography Department of University of Hawaii (1985).
8. Charles L. Mader and Sharon Lukas, "Numerical Modeling of Waianae Harbor," Aha Hulikoa Hawaiian Winter Workshop Proceedings (January 1985).
9. Charles L. Mader, Martin Vitousek, and Sharon Lukas, "Numerical Modeling of Atoll Reef Harbors," Proceedings of the International Symposium on Natural and Man-Made Hazards, Rimouski (1986).
10. Charles L. Mader and Sharon Lukas, "*SWAN* – A Shallow Water, Long Wave Code: Applications to Tsunami Models," Joint Institute for Marine and Atmospheric Research report JIMAR 85–077 (1985).
11. "Oahu Intraisland Ferry System - Draft Environmental Impact Statement," State Department of Transportation, Harbors Division (1988).
12. Charles L. Mader "Modeling Tsunami Flooding," Proceedings of the Pacific Congress on Marine Science and Technology - PACON 90 (1990).
13. G. F. Carrier and H. P. Greenspan, "Water Waves of Finite Amplitude on a Sloping Beach," Journal of Fluid Mechanics Vol 4, 97-109 (1958).
14. G. F. Carrier, "The Dynamics of Tsunamis," Mathematical Problems in the Geophysical Sciences, American Mathematical Society, Vol 1, 157-187 (1971).

TABLE 1

A 1 m High, 48 km Wide Displacement

Time Seconds	Height meters	Bottom Velocity meters/sec	Top Velocity meters/sec
Navier-Stokes Wave -*ZUNI* Code			
0.	1.000	0.0000	0.0000
50.		0.0195	0.0202
100.	0.493	0.0216	0.0231
200.	0.475	0.0216	0.0233
300.	0.464	0.0211	0.0227
400.	0.459	0.0208	0.0224
500.	0.445	0.0203	0.0217
Linear Gravity Wave -*LGW* Code			
0.	1.000	0.0000	0.0000
50.		0.0192	0.0220
100.	0.496	0.0217	0.0238
200.	0.489	0.0214	0.0234
300.	0.478	0.0211	0.0228
400.	0.467	0.0206	0.0222
500.	0.457	0.0201	0.0216
Shallow Water Wave -*SWAN* Code			
0.	1.000	0.0000	0.0000
50.		0.0231	0.0231
100.	0.500	0.0232	0.0232
200.	0.499	0.0232	0.0232
300.	0.500	0.0232	0.0232
400.	0.499	0.0232	0.0232
500.	0.500	0.0232	0.0232

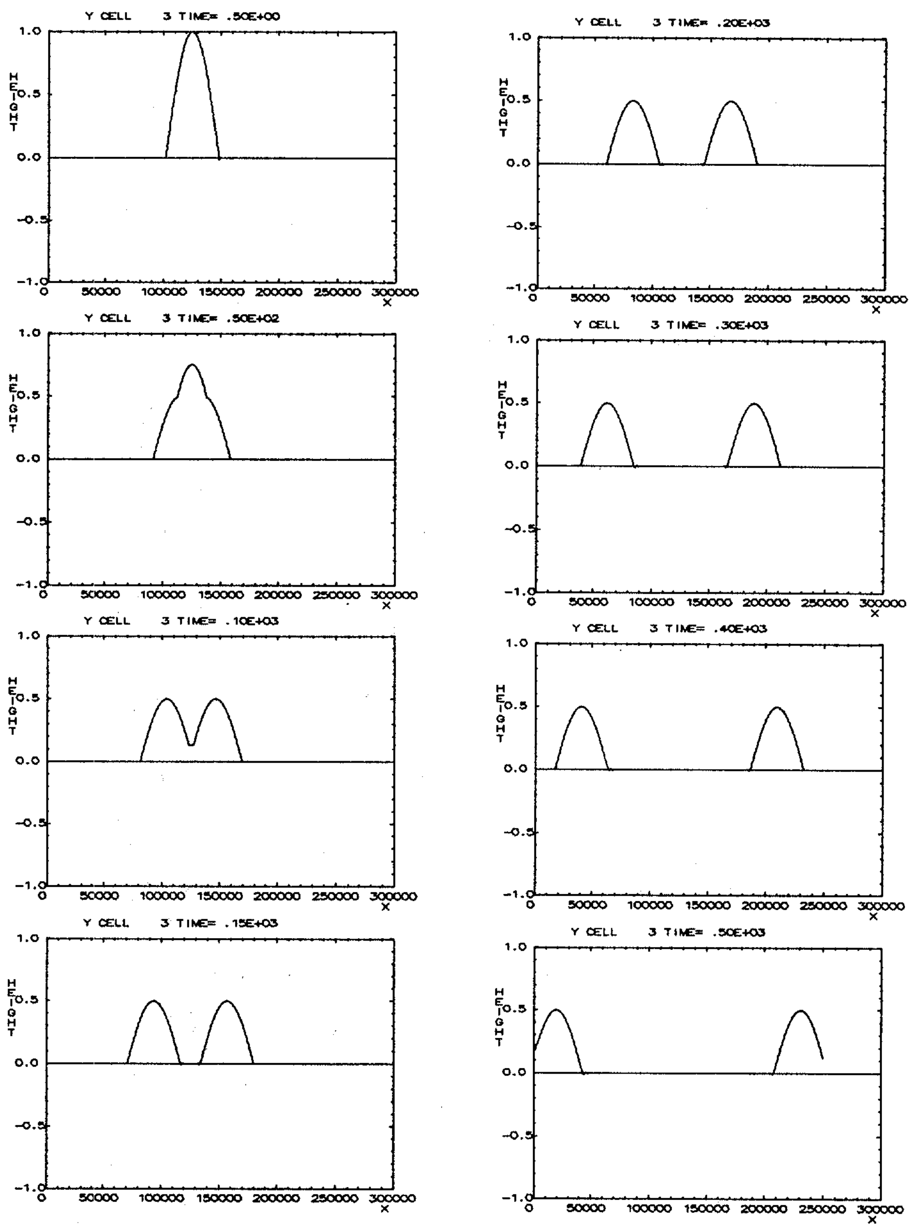

Figure 1. The wave height in meters as a function of distance in meters at various times for a 1 meter high surface displacement with a width of 45 kilometers in 4550 meter deep water for the non-linear shallow water model using the *SWAN* code.

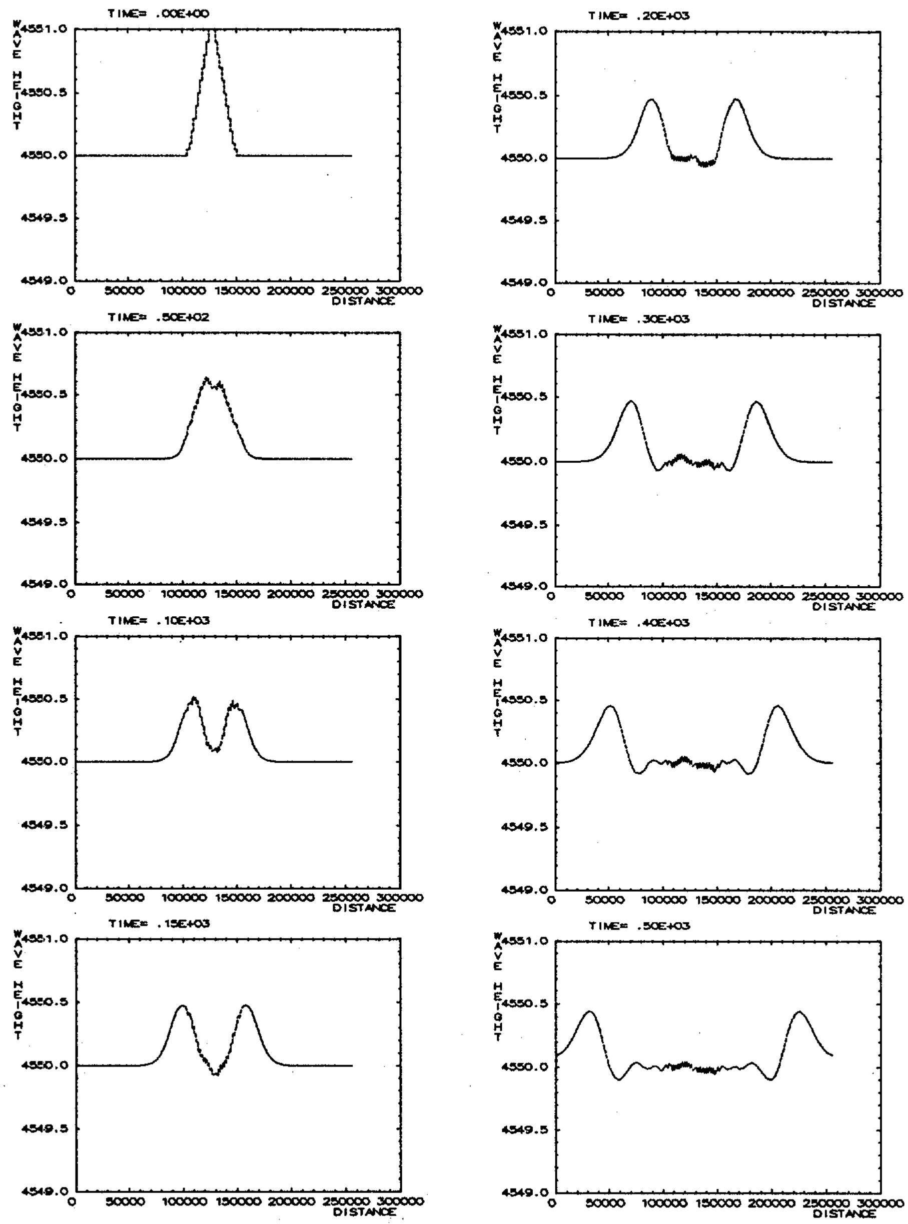

Figure 2. The wave height in meters as a function of distance in meters at various times for a 1 meter high surface displacement with a width of 45 kilometers in 4550 meter deep water for Navier-Stokes water wave model using the *ZUNI* code.

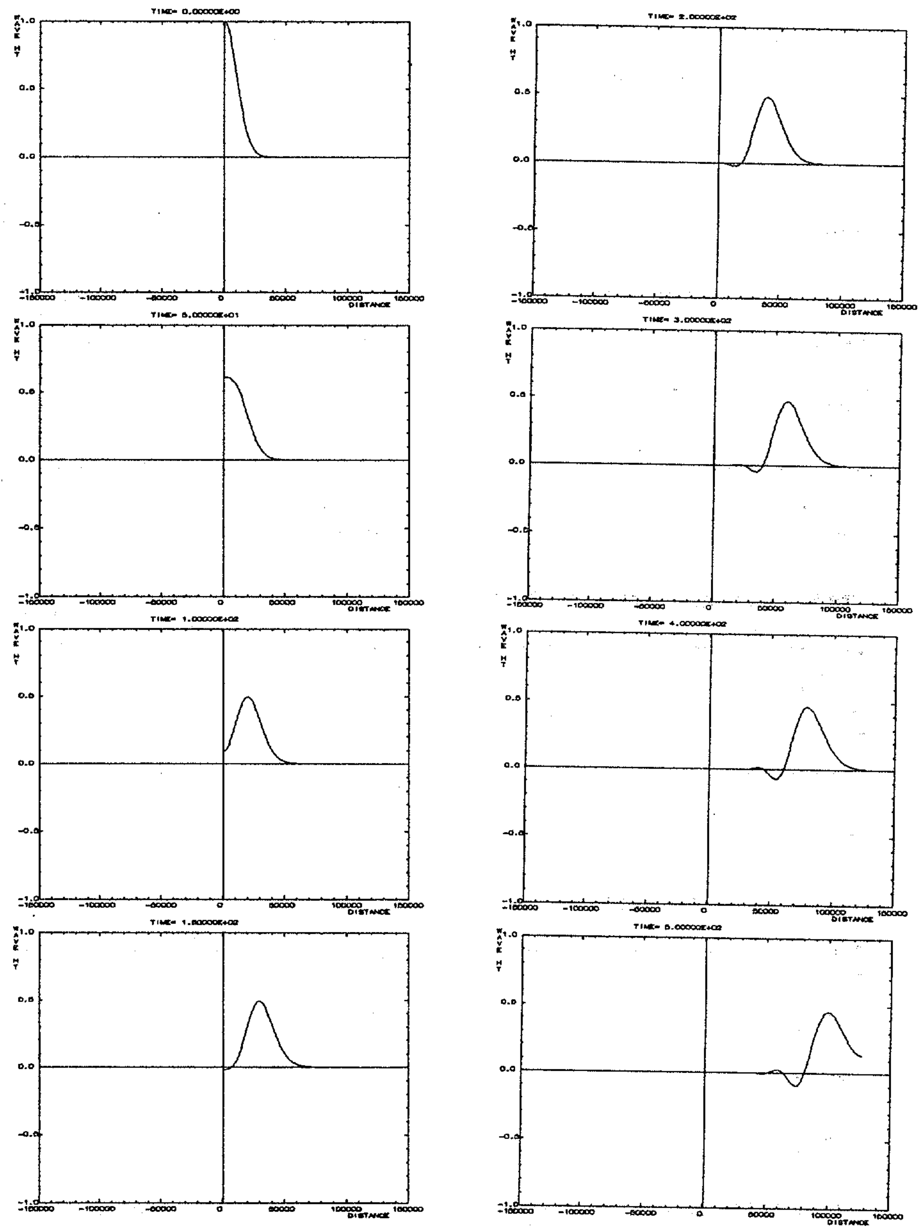

Figure 3. The wave height in meters as a function of distance in meters at various times for a 1 meter high Gaussian displacement with a Gaussian break length of 10 kilometers (equivalent to an Airy half wavelength of 45 kilometers) in 4550 meter deep water for linear gravity water wave model using the *LGW* code.

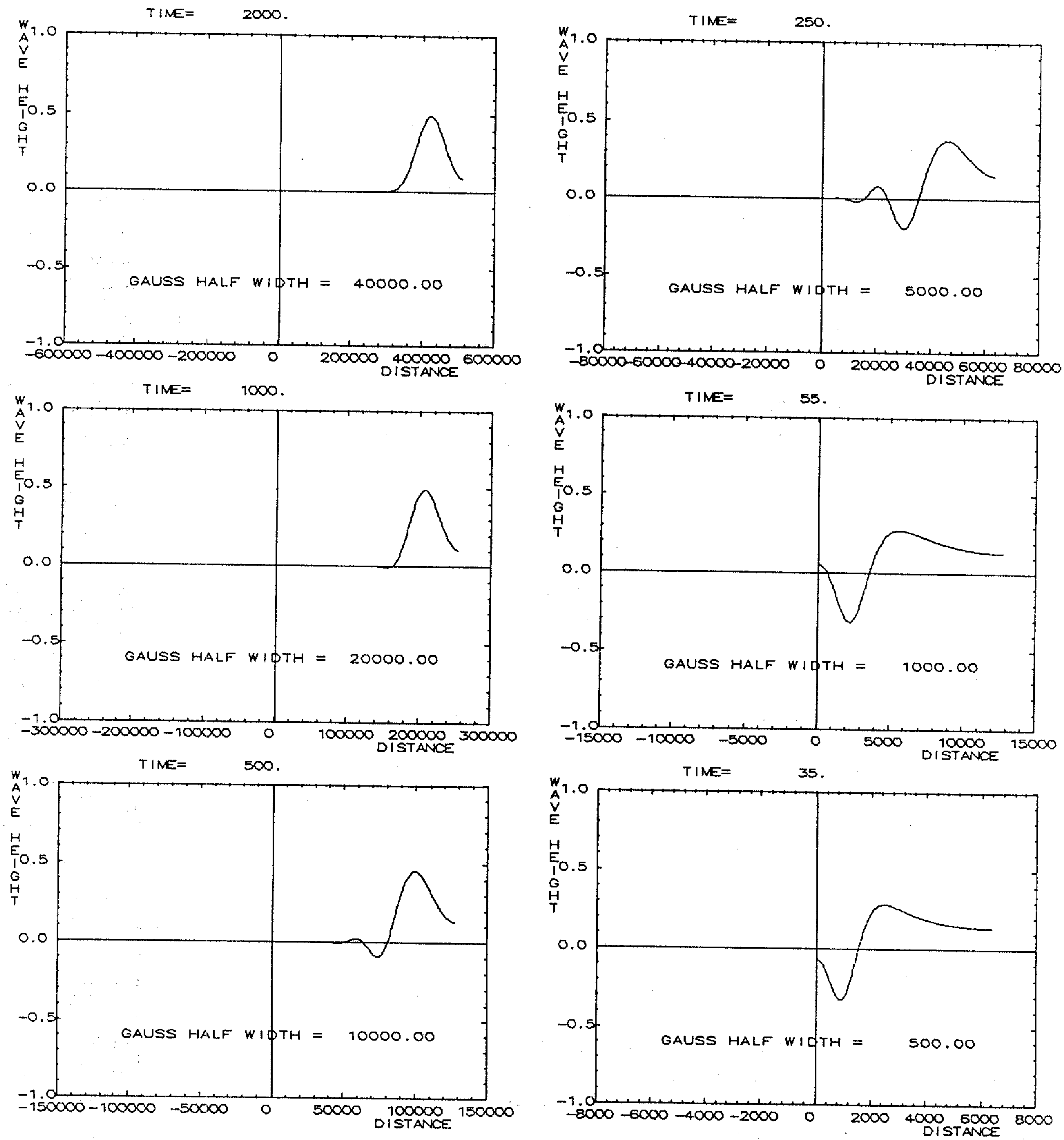

Figure 4. The wave height in meters as a function of distance in meters after the wave has traveled ten times it initial width for a 1 meter high Gaussian displacement with a Gaussian break length of 40, 20, 10, 5, 1, and 0.5 kilometers in 4550 meter deep water for the linear gravity wave model using the LGW code.

NUMERICAL TSUNAMI PROPAGATION STUDY - III

Charles L. Mader
Dennis W. Moore
JTRE - JIMAR Joint Tsunami Research Effort
University of Hawaii, Honolulu, HI., U.S.A.
George F. Carrier
Harvard University, Cambridge, MA., U.S.A.

ABSTRACT

The *SWAN* code solves the nonlinear, shallow water, long wave equations including the effects of friction and flooding. Both the *SWAN* and *ZUNI* code which solves the incompressible Navier-Stokes equations were used to study the propagation of a tsunami wave from an initial sea surface displacement similar to the propagation of a tsunami wave from Alaska or the U.S. West Coast to Hawaii. The propagation of a tsunami wave was also modeled using two-dimensional linear gravity wave theory.

If the initial displacement is approximately Gaussian and the wavelength is very long compared to the depth, the tsunami wave does not disperse or decay appreciably and similar tsunami waves propagate for all three methods. Two tsunami waves traveling in opposite directions formed that were the sum of the original surface displacement. However dispersion effects resulted in Navier-Stokes and linear gravity waves with decreasing amplitudes, front slopes, and followed by a train of smaller waves.

With decreasing periods and wavelengths, the discrepancy between the shallow water and the Navier-Stokes and linear gravity waves formed from initial sea surface displacement increases. This discrepancy as a function of the size of the tsunami source relative to the depth and distance or time of tsunami propagation is characterized.

Most tsunami waves that have been observed after traveling across the ocean have periods longer than 10 minutes because shorter waves are so dispersive that they decay as they propagate long distances.

Introduction

The magnitude of the tsunami hazard at any land site depends upon the expected extent of flooding of the land by tsunamis at the site, the expected water velocities and the exposure of persons and property within the potential flood zone. The development of numerical models to describe tsunami wave generation, propagation and interaction with complicated topography such as bays or harbors and the resulting flooding has advanced to the stage where they are useful tools for determining the tsunami hazard in local regions. A numerical study of the flooding of Hilo, Hawaii by the tsunamis of April 1, 1946, May 23, 1960 and March 28, 1964 was described in reference 1.

The relative importance of the characteristics of the tsunami and the topography in and between the available models is being determined. The characterization of the tsunami flooding problem is a large and continuing effort. In this paper we describe the third study in our parameteric study of numerical and analytical tsunami models. The first study was described in reference 2. The effect of tsunami wave period, amplitude, bottom slope angle and friction on tsunami shoaling and flooding was investigated using a shallow water and a Navier-Stokes numerical model. The study showed higher wave shoaling and flooding for waves interacting with steeper slopes, for waves with longer periods and for waves from deeper water. The shallow water waves shoal higher, steeper and faster than the Navier-Stokes waves. The differences increase as the periods become shorter and slopes less steep with large differences for periods less than 500 seconds and slopes less than 2 percent.

The second study was described in reference 3. We examined the formation of a tsunami wave from an initial sea surface displacement similar to those obtained from earthquakes that have generated tsunami waves. Given an initial sea surface displacement, the characteristics of the tsunami wave formed using the non-linear shallow water model, the incompressible Navier-Stokes model, and the analytical linear gravity wave model were compared. With decreasing periods and wavelengths, the discrepancy between the shallow water and the Navier-Stokes and linear gravity waves formed from initial sea surface displacement increased. It was concluded that the shallow water model should be used only for systems with initial surface displacements at least ten times wider than the depth.

The Shallow Water Numerical Model

The *SWAN* code solves the incompressible, shallow water, long wave equations. It is described in detail in the monograph *Numerical Modeling of Water Waves* [5] .

The incompressible, shallow water, long wave equations solved by the *SWAN* code are

$$\frac{\partial U_x}{\partial t} + U_x \frac{\partial U_x}{\partial x} + U_y \frac{\partial U_x}{\partial y} + g \frac{\partial H}{\partial x} = F U_y + F^{(x)} - g \frac{U_x (U_x^2 + U_y^2)^{1/2}}{C^2 (D + H - R)} ,$$

$$\frac{\partial U_y}{\partial t} + U_x \frac{\partial U_y}{\partial x} + U_y \frac{\partial U_y}{\partial y} + g \frac{\partial H}{\partial y} = -F U_x + F^{(y)} - g \frac{U_y (U_x^2 + U_y^2)^{1/2}}{C^2 (D + H - R)} ,$$

$$\frac{\partial H}{\partial t} + \frac{\partial (D + H - R) U_x}{\partial x} + \frac{\partial (D + H - R) U_y}{\partial y} - \frac{\partial R}{\partial t} = 0 ,$$

where U_x is velocity in x direction, U_y is velocity in y direction, g is gravitational acceleration, t is time, H is wave height above mean water level, R is bottom motion, F is Coriolis parameter, C is coefficient of DeChezy for bottom friction, $F^{(x)}, F^{(y)}$ are forcing functions of wind stress in x and y direction, and D is depth.

Flooding is described using positive values for depths below normal water level and negative values for elevations above normal water level. Only positive values of the $(D + H)$ terms in the above equations are permitted. This method results in both flóoding and receding surfaces being realistically described by the *SWAN* code.

The Navier-Stokes Numerical Model

The two-dimensional time dependent Navier-Stokes equations for incompressible flow solved by the *ZUNI* code are

$$\frac{\partial U_x}{\partial x} + \frac{\partial U_y}{\partial y} = 0 \, ,$$

$$\frac{\partial U_x}{\partial t} + U_x \left(\frac{\partial U_x}{\partial x} \right) + U_y \left(\frac{\partial U_x}{\partial y} \right) = -\frac{1}{\rho_o} \frac{\partial P}{\partial x} + g_x + \frac{\mu}{\rho_o} \left(\frac{\partial^2 U_x}{\partial x^2} + \frac{\partial^2 U_x}{\partial x \partial y} \right) \, ,$$

$$\frac{\partial U_y}{\partial t} + U_x \left(\frac{\partial U_y}{\partial x} \right) + U_y \left(\frac{\partial U_y}{\partial y} \right) = -\frac{1}{\rho_o} \frac{\partial P}{\partial y} + g_y + \frac{\mu}{\rho_o} \left(\frac{\partial^2 U_y}{\partial y \partial x} + \frac{\partial^2 U_y}{\partial y^2} \right)$$

where P is pressure and μ is the viscosity coefficient. A partial cell treatment that allows a rigid free slip obstacle to be placed through cell diagonals is included. The desired boundary slope is obtained by choosing the appropriate aspect ratio for the cells of the mesh. Thus, the numerical technique can be used to calculate wave run-up on exposed beaches in addition to submerged beaches. The details of the calculational procedure are described in reference 5.

The detailed Navier-Stokes numerical simulation of gravity waves that resemble the profile of actual tsunami waves was first achieved in reference 4. The interaction of tsunami waves with slopes that resembled the continental slope and shelf was simulated. Wave heights were calculated to increase by a factor of 4 as they shoaled up a 6.66 percent continental slope.

The *ZUNI* code was used to model the effect of submerged barriers on waves as described in references 4 and 5. The calculated transmission coefficients (ratio of wave height inside to height outside barrier) from experimental underwater barrier data were reproduced by the numerical model. Underwater barriers reflect significant amounts of the tsunami energy approaching a bay or harbor.

Water waves generated by explosions which produce bubbles underwater and cavities in the water surface have been described using the *ZUNI* code in references 4 and 5. The experimentally observed waves generated by cavities from explosions were deep water waves which were reproduced using the *ZUNI* code but not by the *SWAN* code.

The interaction of waves with submerged barriers and explosively generated water waves can not be described using the shallow water model since significant features of the flow are characteristic of deep water waves.

The Linear Gravity Wave Model

The analytical methods for solving the linear gravity wave model are described by Carrier in references 6 and 7. The two-dimensional linear gravity wave with a Gaussian, a square wave or a time dependent Gaussian displacement is solved using Fourier transforms by the *LGW* code for any time of interest. The wave description is obtained for any uniform depth, density, gravity and Gaussian break width or square wave half-width. The wave height, vertical and horizontal velocities, and pressure are calculated at any depths desired. The distance scale is chosen to be a tenth of the Gaussian break width so that a wave half-width is described by about 50 space increments. Since the model is symmetrical about the center of the initial displacement, only half of the wave profile is calculated.

Tsunami Propagation Study - *SWAN* Model

A 1 meter high Airy half-wave surface displacement with a width of 45 kilometers in 4550 meter deep water was studied. This approximates within cell resolution a Gaussian wave with a Gaussian break width of 10 kilometers. The calculations were performed on an IBM PS/2 Model 95 computer using a version of the *SWAN* code that includes flooding and MCGRAPH graphics for the OS/2 operating system. Calculations were performed using a 250 meter wide mesh of 32,000 by 4 cells and at 0.5 second intervals.

The wave height in meters as a function of distance is shown in Figure 1 at half hour intervals. The initial surface displacement separates into two shallow water waves with a height of 0.5 meter and width of 45 kilometers.

The non-linear feature of the shallow water model included in the *SWAN* code results in a small trailing wave with an amplitude of less than 0.01 meter. The peak wave amplitude remains nearly constant as the wave propagates.

Tsunami Propagation Study - *ZUNI* Model

A 1 meter high approximately (within cell resolution) Gaussian surface water displacement with Gaussian break width of 10 km (which is equivalent to an Airy wave with a half-wavelength of 45 kilometers) in 4550 meter deep water as it traveled for 3 hours was studied. The calculations for this geometry were performed with 15 cells in the Y or depth direction and up to 13,600 cells in the X or distance direction. The calculation required 231,200 cells and over 2.5 million mesh quantities.

The cells were rectangles 450 meters high in the Y direction and 4000 meters long in the X direction. The time increment was 3 seconds. The water level was placed at 4550 meters or 50 meters up into the eleventh cell. The viscosity coefficient used was 0.02 poise, a value representative of the actual viscosity for water. The viscosity did not significantly affect the results. These results are an extension of those described in references 2 thru 5.

The calculations were performed on an IBM PS/2 Model 95 computer using a special version of the *ZUNI* code that includes flooding and MCGRAPH graphics for the OS/2 operating system.

The wave height in meters as a function of distance is shown in Figure 2 at various times. The initial surface displacement separates into two nearly shallow water waves with a height of 0.5 meter and width of 45 kilometers. At 100 seconds the two waves have formed and the vertical velocity at the center of the wave is 0.0231 meters/sec. at the top of the wave to 0.2158 meters/sec. near the bottom of the wave. An Airy wave with a 0.5 meter half-width, 90 km wavelength in 4550 meters of water has a vertical velocity of 0.0235 to 0.0226 meters/sec. at the center of the wave. The Airy wave speed is 208.36 meters/sec. and the group velocity is 202.89 meters/sec.

As the wave propagates the wave height decreases, the slope of the front of the wave becomes smaller, and a train of small waves form behind the main wave. After the wave has propagated for 3 hours and over 2.3 megameters, the wave height has decreased to 0.20 meters. A train of waves has developed behind the main wave with maximum negative amplitude of 0.14 meter and positive amplitude of 0.11 meter.

Tsunami Propagation Study - *LGW* Model

A 1 meter high Gaussian surface water displacement with a Gaussian break width of 10 km (which is equivalent to an Airy wave with a half- wavelength of 45 kilometers) propagating for 3 hours in 4550 deep water was studied. The wave height in meters as a function of distance is shown in Figure 3 at various times. The initial surface displacement separates into two nearly shallow water waves with a height of 0.5 meters and length of 45 kilometers.

The analytical linear gravity wave calculations were performed using up to 16,384 points. The wave profile was calculated for each time selected. The calculations were performed on an IBM PS/2 Model 95 computer using a version of the *LGW* code which uses the MCGRAPH graphics on the OS/2 operating system.

As the wave propagates the wave height decreases, the slope of the front of the wave becomes smaller, and a train of small waves form behind the main wave. After the wave has propagated for 3 hours and over 2.3 megameters, the wave height has decreased to 0.22 meters. A train of waves has developed behind the main waves with maximum negative amplitude of 0.16 meter and positive amplitude of 0.12 meter. The peak height of the linear gravity wave decreases slower and the following wave train heights are higher than for the Navier-Stokes wave. The peak height of the Navier-Stokes wave is about 10 percent less than the linear gravity wave peak height after three hours of travel. This difference is an order of magnitude less than the difference between either wave and the shallow water wave height which is more than twice as high. The period of the waves in the following wave train are similar; however the amplitudes are slightly higher for the linear gravity wave train. These results support the use of the linear gravity wave model for studying the effect of various wavelength to depth ratios and of tsunami propagation for longer distances and times.

The linear gravity wave model was used to investigate wave propagation from initial surface displacements of width to depth ratios of 40 to 5.0 (Gaussian break widths of 40 to 5. kilometers) in 4550 meters deep water. The wave height after the wave had traveled for 0.5, 2.0, 5.0 and 10.0 hours for depth ratios of 40, 20, 10, and 5 are shown in Figure 4. The Airy half-wave-length and half-wave-period equivalents for a break width of 5 is 23 kilometers and about 1.8 minutes, a break width of 10 is 46 kilometers and 3.5 minutes, a break width of 20 is 90 kilometers and 7 minutes, and for a break width of 40 is 180 kilometers and 14 minutes.

After traveling for 10 hours and 7.6 megameters, the peak wave amplitude for the 40 break width wave decreased from 0.5 to 0.42 meters, the 20 break width wave amplitude decreased to 0.28 meters, the 10 break width wave amplitude decreased to 0.16 meters, and the 5 break width wave amplitude decreased to 0.08 meters. The addition of non-linear effects will lower these heights so these are upper bounds on the peak wave amplitude.

Conclusions

The non-linear shallow water wave becomes less realistic the further it travels from its source and the smaller the width to depth ratio. Non-linear shallow water models are adequate for large wave length and long period tsunamis such as generated by the 1964 Alaskan or the 1960 Chile earthquakes where the periods were about 30 minutes and wavelength to depth ratio in the deep ocean was greater than 80. Tsunami wave propagation from and generation by earthquakes with small areas and periods of a few minutes are not realistically described using shallow water models. Either the linear gravity wave model or better the Navier-Stokes model should be used for accurate modeling of long distance propagation of tsunamis with small (less than 40) width to depth ratios.

Most tsunami waves that have been observed after traveling across the ocean have periods longer than 10 minutes. These studies support the postulate discussed in reference 5 that this is because the shorter wave length tsunamis are so dispersive that as they propagate long distances, their amplitude decreases by an order of magnitude.

Only part of the parameteric region of interest for tsunami generation, propagation and flooding has been investigated, particularly for the Navier-Stokes model. Since three-dimensional Navier-Stokes solutions to tsunami problems currently have limited practical application, most tsunami flooding studies need to be performed using the shallow water model. These studies permit us to determine the parameteric region where the shallow water model can be useful.

The development and application of three-dimensional Navier-Stokes models including a realistic bottom friction treatment will be required for significant improvement in our ability to realistically model tsunami generation, propagation and flooding.

Acknowledgments

The author gratefully acknowledge the contributions of G. D. Curtis, and H. G. Loomis of the University of Hawaii, Z. Kowalik of the University of Alaska, T. S. Murty of the Institute of Ocean Sciences, and E. N. Bernard of the Pacific Marine Environmental Laboratory.

References

1. Charles L. Mader and George D. Curtis, "Modeling Hilo, Hawaii Tsunami Inundation," Science of Tsunami Hazards, Vol 9, 85-94 (1991).
2. Charles L. Mader, "Numerical Tsunami Flooding Study - I ," Science of Tsunami Hazards, Vol 8, 79-96 (1990).
3. Charles L. Mader, Dennis W. Moore, and George F. Carrier, "Numerical Tsunami Source Study - II ," Science of Tsunami Hazards, Vol 11, - (1993).
4. Charles L. Mader, "Numerical Simulation of Tsunamis," Journal of Physical Oceanography, Vol. 5, pp. 75–82 (1975).
5. Charles L. Mader *Numerical Modeling of Water Waves,* University of California Press, Berkeley, California (1988).
6. G. F. Carrier and H. P. Greenspan, "Water Waves of Finite Amplitude on a Sloping Beach," Journal of Fluid Mechanics Vol 4, 97-109 (1958).
7. G. F. Carrier, "The Dynamics of Tsunamis," Mathematical Problems in the Geophysical Sciences, American Mathematical Society, Vol 1, 157-187 (1971).

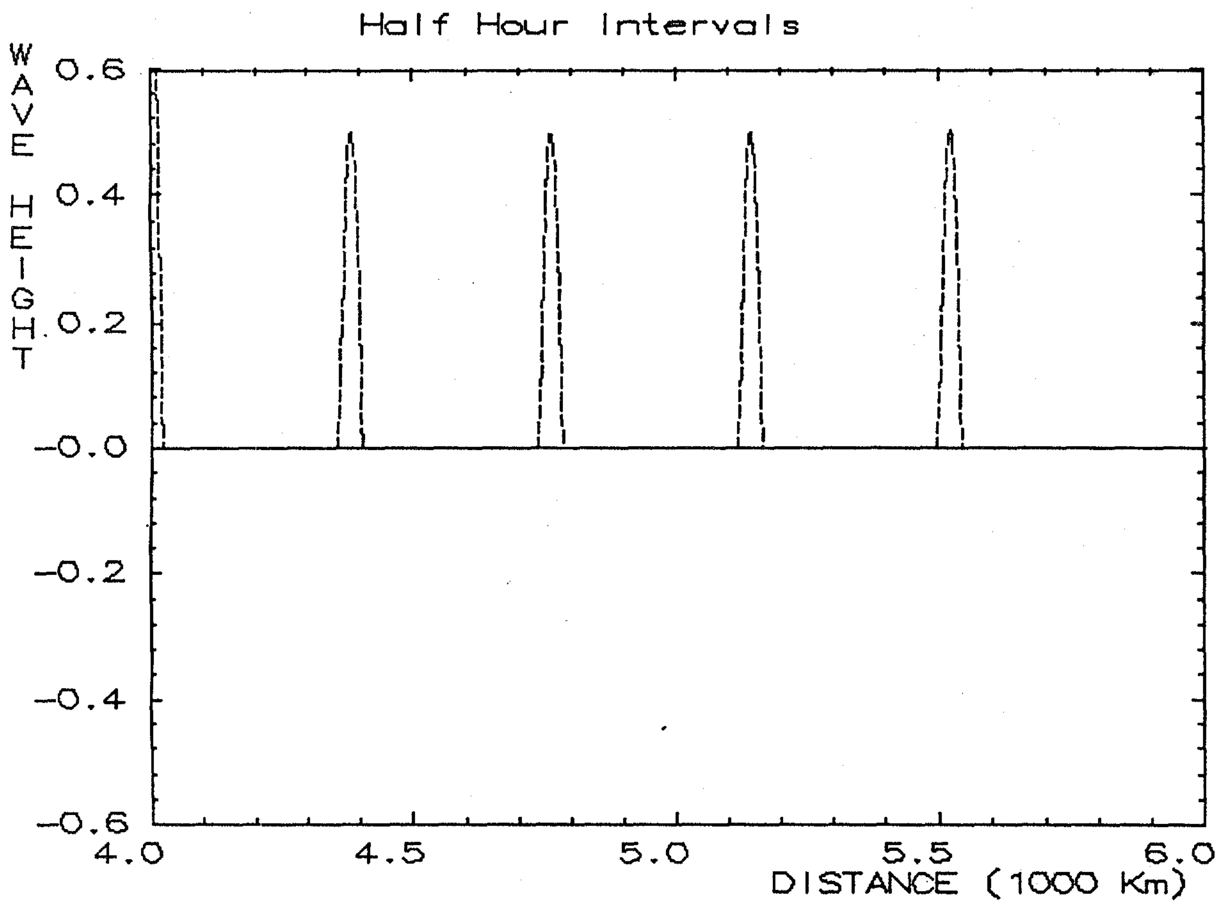

Figure 1. The wave height in meters as a function of distance in meters at half hour intervals for a 1 meter high surface displacement with a width of 45 kilometers in 4550 meter deep water for the non-linear shallow water model using the *SWAN* code.

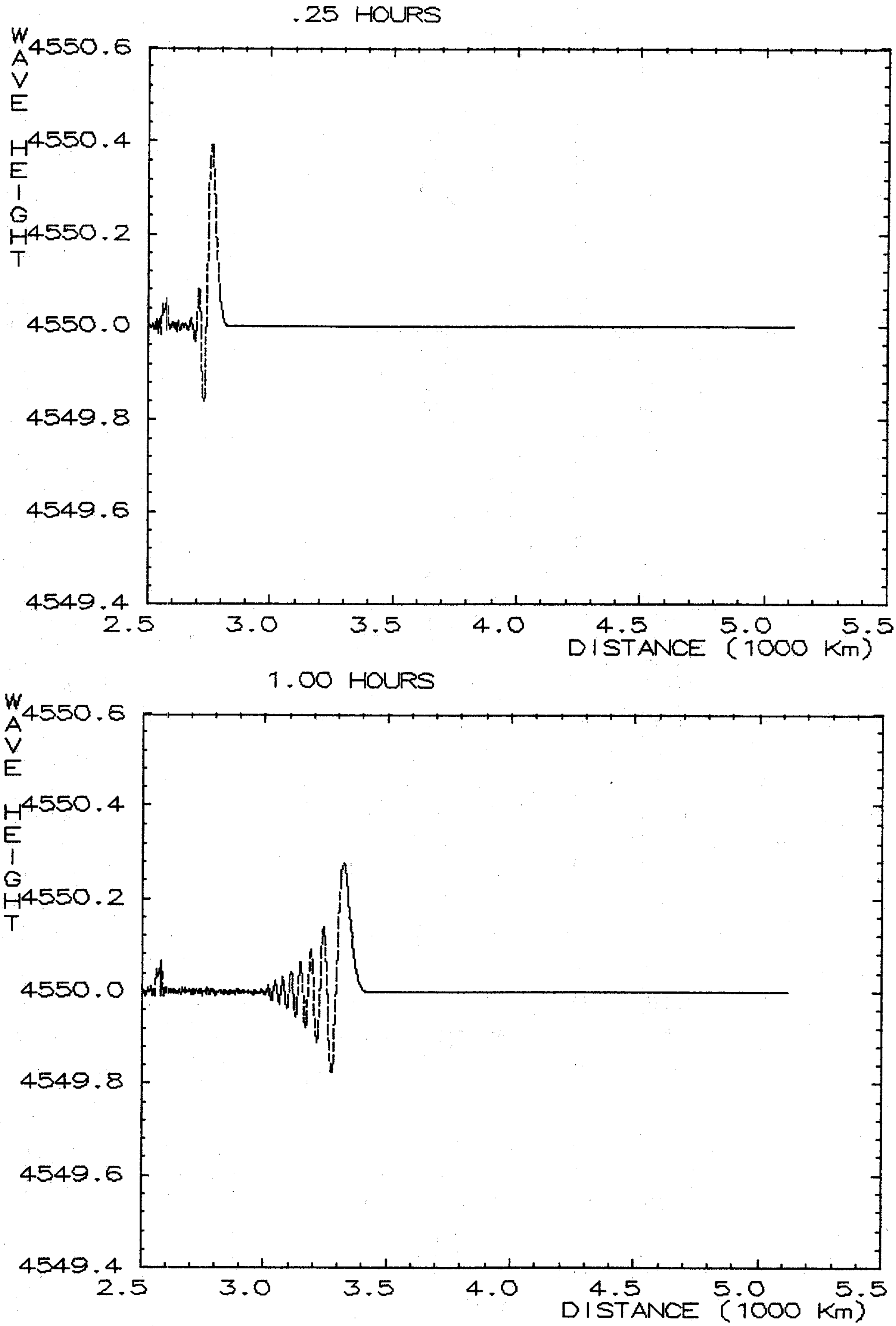

Figure 2. The wave height in meters as a function of distance in meters at various times for a 1 meter high surface displacement with a width of 45 kilometers in 4550 meter deep water for Navier-Stokes water wave model using the *ZUNI* code.

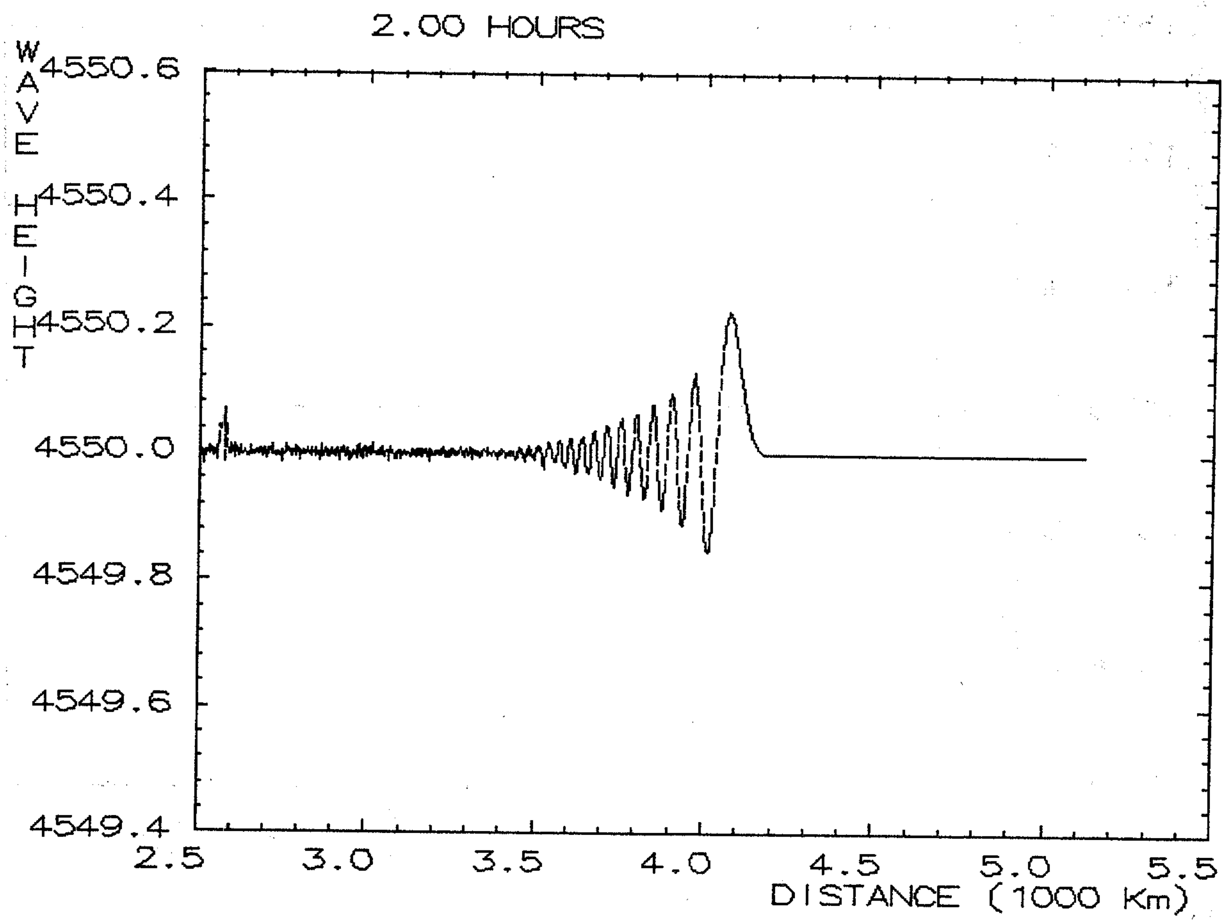
2.00 HOURS
WAVE HEIGHT
4550.6
4550.4
4550.2
4550.0
4549.8
4549.6
4549.4
2.5
3.0
3.5
4.0
4.5
5.0
5.5
DISTANCE (1000 Km)

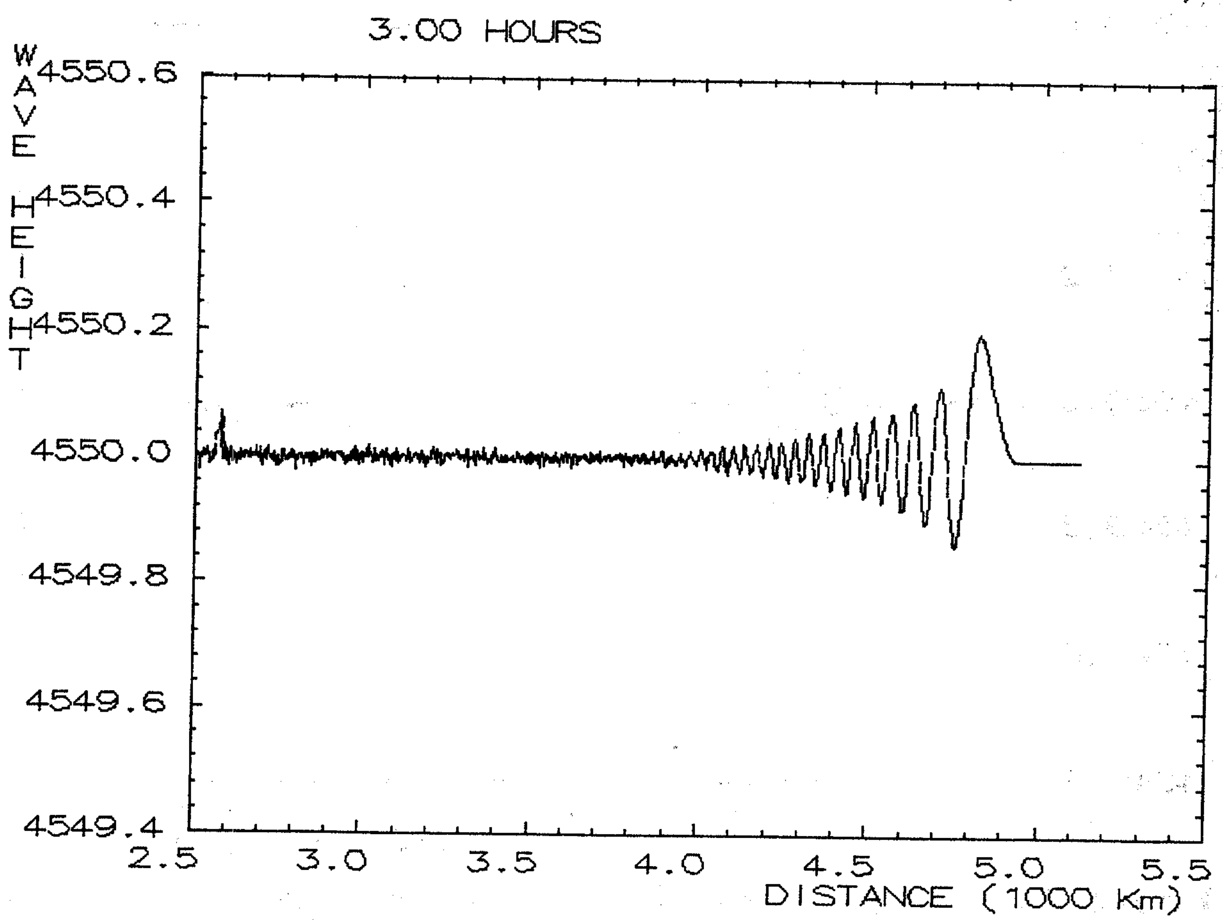
3.00 HOURS
WAVE HEIGHT
4550.6
4550.4
4550.2
4550.0
4549.8
4549.6
4549.4
2.5
3.0
3.5
4.0
4.5
5.0
5.5
DISTANCE (1000 Km)

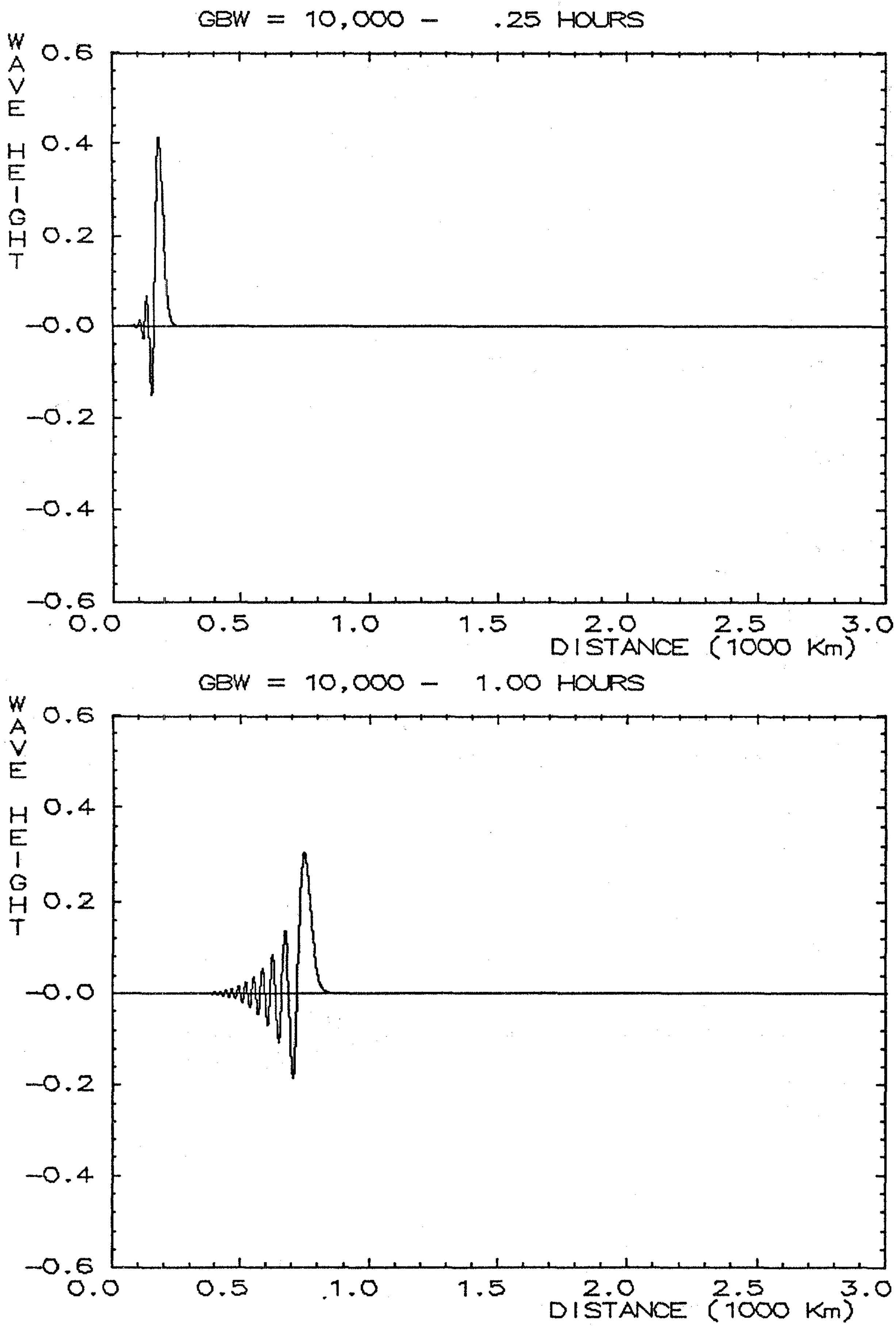

Figure 3. The wave height in meters as a function of distance in meters at various times for a 1 meter high surface displacement with a width of 45 kilometers in 4550 meter deep water for linear gravity wave model using the *LGW* code.

GBW = 10,000 - 2.00 HOURS

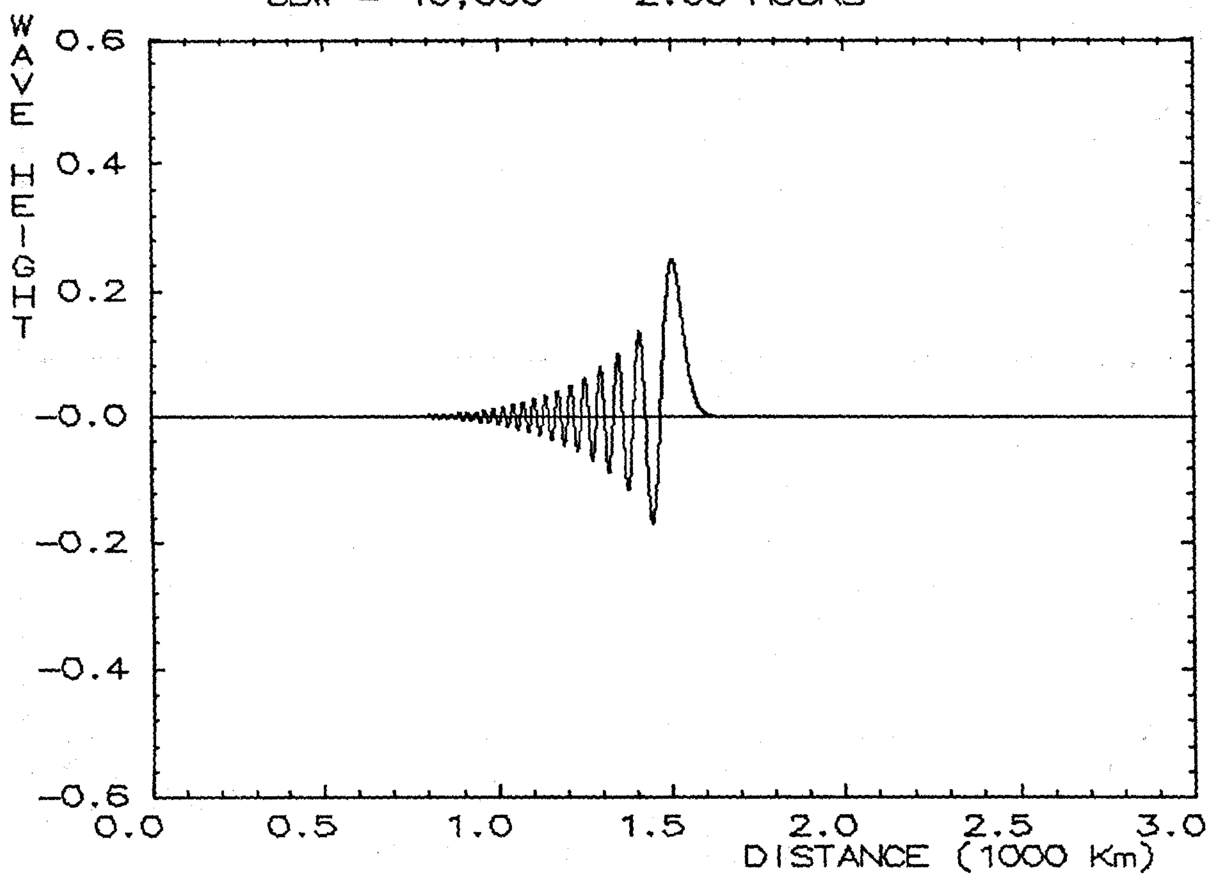

GBW = 10,000 - 3.00 HOURS

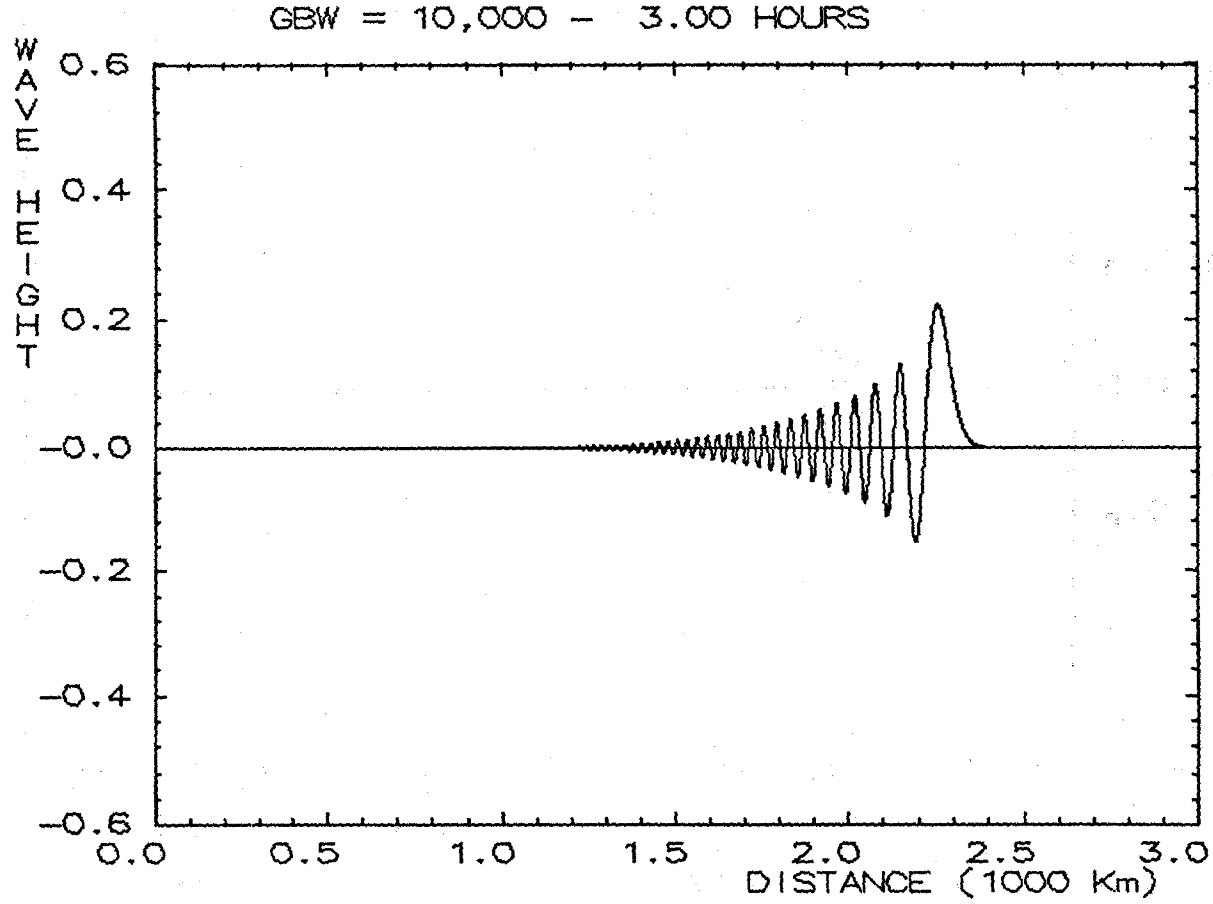

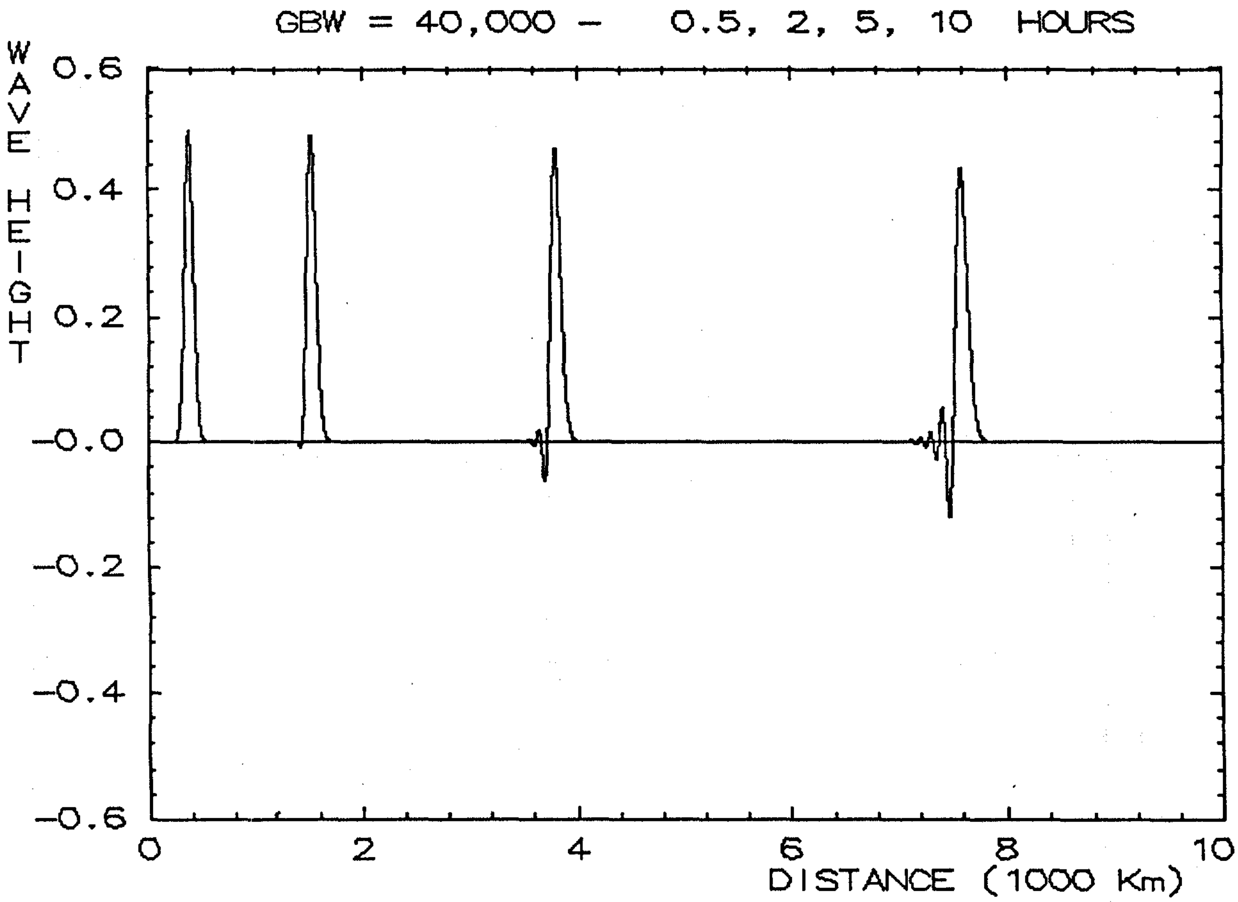

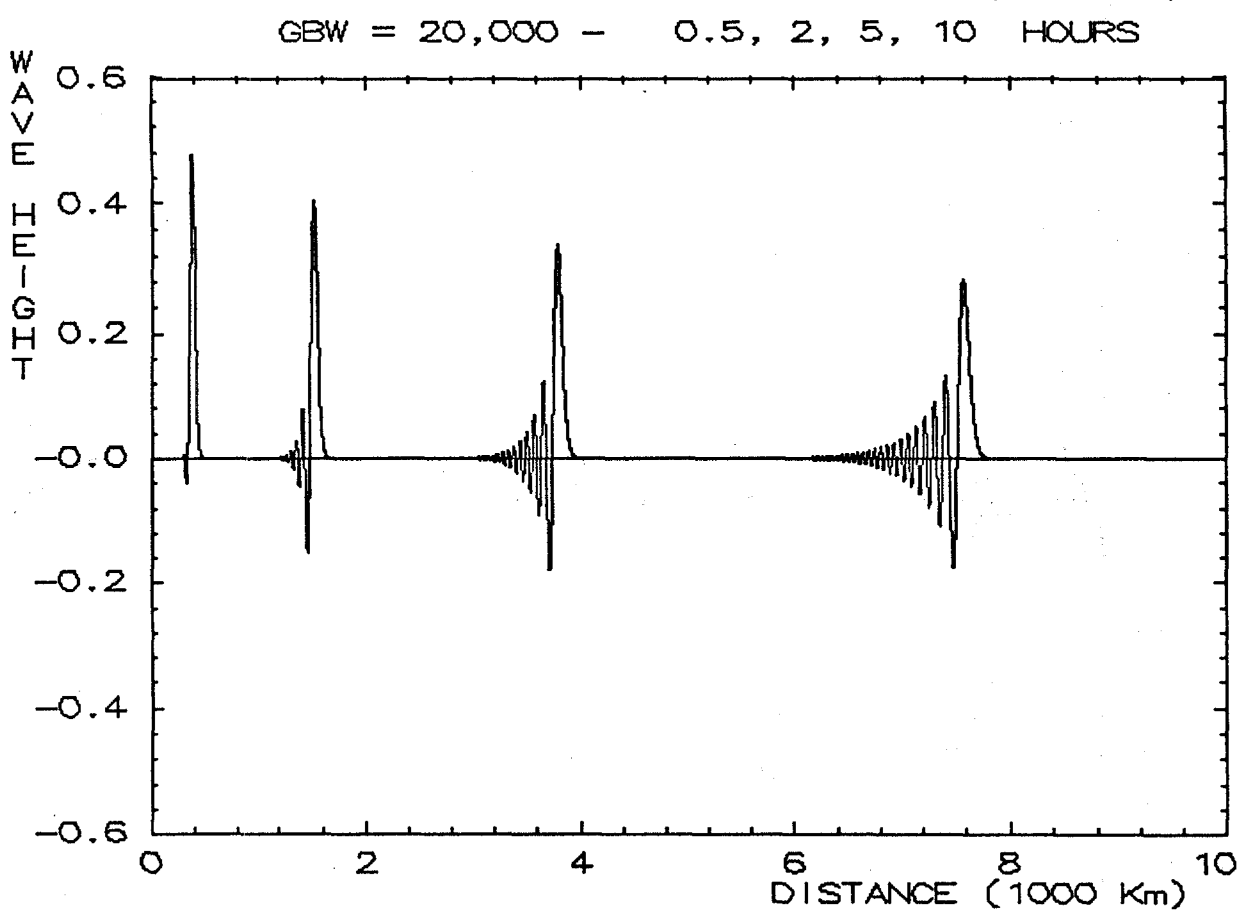

Figure 4. The wave height in meters as a function of distance in meters after the wave has traveled up to 10 hours and 7.6 megameters for a 1 meter high Gaussian displacement with a Gaussian break length of 40, 20, 10, and 5 kilometers in 4550 meter deep water for the linear gravity wave model using the *LGW* code.

GBW = 10,000 - 0.5, 2, 5, 10 HOURS

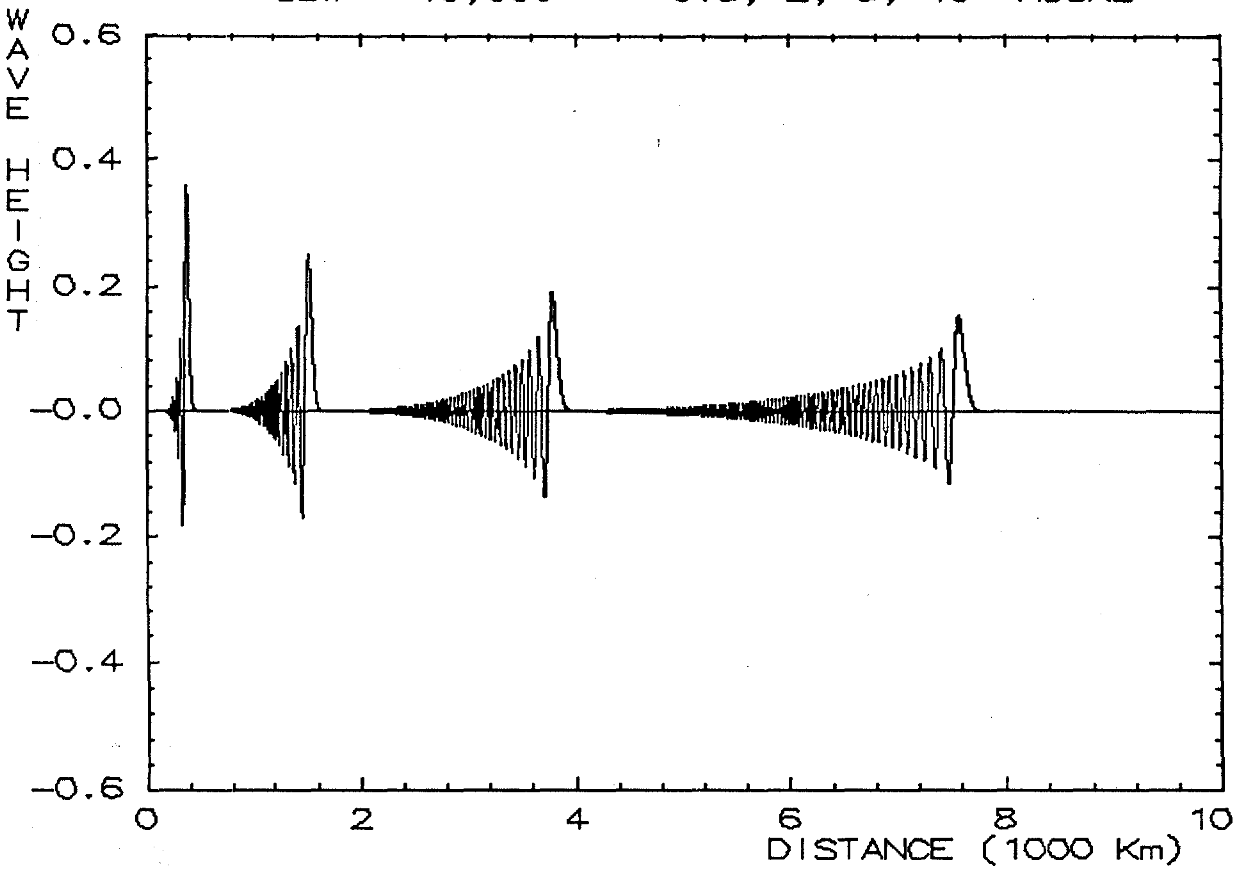

GBW = 5,000 - 0.5, 2, 10 HOURS

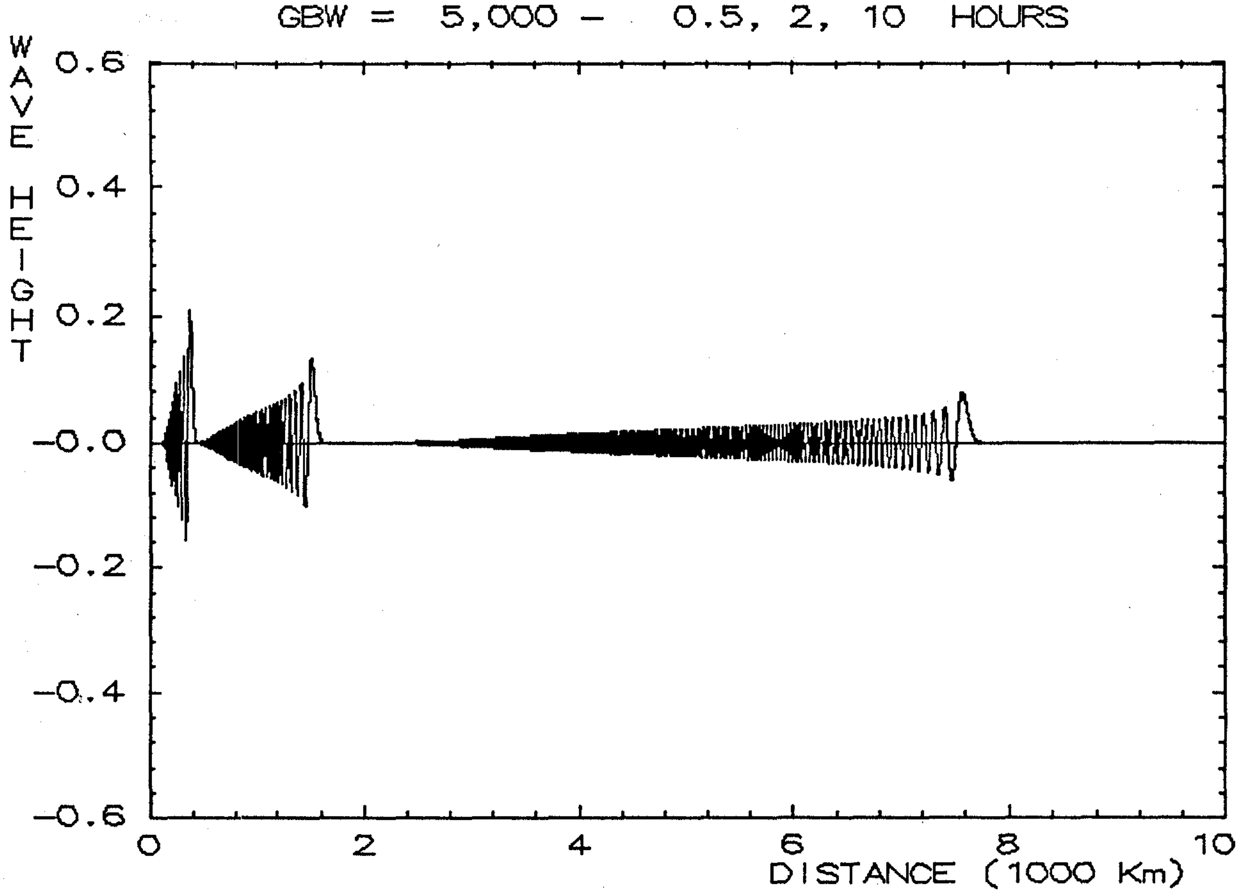

SHALLOW WATER VALIDITY

SOURCE - WIDTH 10 TIMES LONGER DEPTH

PROPAGATION - WIDTH 40 TIMES DEPTH
IN DEEP (5 KM) OCEAN - 15 MIN PERIOD

RUNUP - GREATER THAN 15 MIN PERIOD

FLOODING - GREATER THAN 10 MIN PERIOD

FLOODING - GREATER THAN 2 PERCENT SLOPE

MODELING THE 1992 NICARAGUA TSUNAMI

Charles L. Mader
Senior Fellow, JTRE - JIMAR Tsunami Research Effort
University of Hawaii, Honolulu, HI., U.S.A.

ABSTRACT

The generation and propagation of a tsunami off the coast of Nicaragua on September 2, 1992 was modeled for two possible sources. The tsunami wave was observed to be a single half-wave with a half-wave period of 7 minutes and a height of 10 meters. The modeling was performed using the *SWAN* code which solves the nonlinear long wave equations.

The tsunami generation and propagation was modeled using a 1.25 minute grid for the Nicaraguan coast. Two possible sources were examined. The earthquake sea floor displacement and a large landslide recently located seaward of the earthquake epicenter were examined. The earthquake sea floor displacement with a maximum displacement of 18 meters was calculated to reproduce the observed single half-wave tsunami period and height. The landslide produced a train of waves with periods of less than one minute which suggests that the landslide was not the primary generation source for the tsunami wave.

MODELING

The generation and propagation of the tsunami wave of September 2, 1992 off the coast of Nicaragua was modeled using a 1.25 degree grid of the topography. The modeling was performed using the *SWAN* non-linear shallow water code which includes Coriolis and frictional effects. The *SWAN* code is described in Reference 1. The calculations were performed on 50 Mhz 486 personal computers with 16 megabytes of memory. The 5 minute topography from the NOAA ETOPO 5 minute grid of the earth was used to generate the 1.25 minute grid by successive interpolation. The grid was 285 by 278 cells and the time step was 4 seconds. The finer grid was essential to obtain adequately resolved earthquake generated waves in shallow water near the shore line. The finer grid was also required to resolve the short period waves generated by the landslide source.

The earthquake parameters used for the September 2, 1992 Nicaragua tsunami are shown in the following table. The sea floor displacement contours are shown in Figure 1.

Earthquake Parameters

Latitude	11.7 N
Longitude	87.4667 S
Length	120 Km
Width	75 Km
Depth	20 Km
Dip	15 deg
Rake	91 deg
Strike	-57 deg

The landslide parameters used were obtained from recent NOAA investigations of the sea floor near the earthquake. The previous survey was ten years earlier, so it can only be assumed that the observed landslide was triggered by the earthquake. The observed sea floor change was a depression of 200 meters over a region of 4 by 10 kilometers located south-west of the earthquake epicenter. Even with the 1.25 degree grid, the source resolution was only 2 by 5 cells with an initial displacement of 200 meters in about 3000 meters of water. The tsunami wave was observed to be a single half-wave with a half-wave period of 7 minutes and a height of 10 meters.

The propagation of the tsunami wave from the earthquake source is shown in Figure 2. The wave height as a function of time is shown in Figure 3 at a location near the shore and 220 kilometers West of the earthquake epicenter. The half-wave period is approximately 7 minutes with a single-half wave amplitude of 10 meters near the shore.

The propagation of the tsunami wave from the landslide source is shown in Figure 4. The wave height as a function of time is shown in Figure 5 at a location toward the shore and 140 kilometers West of the landslide. The wave period is approximately 70 seconds the calculated tsunami is a train of waves of amplitudes of up to 10 meters toward the shore.

The earthquake sea floor displacement with a maximum displacement of 18 meters was calculated to reproduce the observed single half-wave tsunami period and height. The landslide produced a train of waves with periods much shorter than observed. This indicates that the landslide was not the primary source for the tsunami wave.

Acknowledgments

The author acknowledges the contributions of George Curtis, Dr. Gus Furamoto, Dr. Doak Cox, Dr. Dennis Moore, Dr. E. N. Bernard, Dr. Frank Gonzalez, George Nabeshima, and the Pacific Tsunami Warning Center.

REFERENCES

1. Charles L. Mader *Numerical Modeling of Water Waves,* University of California Press, Berkeley, California (1988).

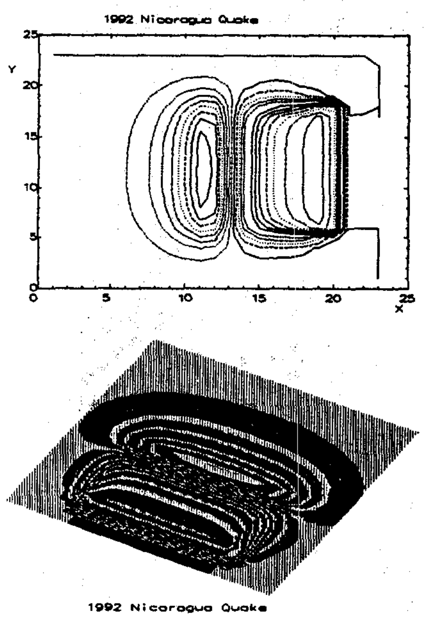

Figure 1. The sea floor displacements for the Nicaragua earthquake of September 2, 1992. The contour interval is 1.5 meters.

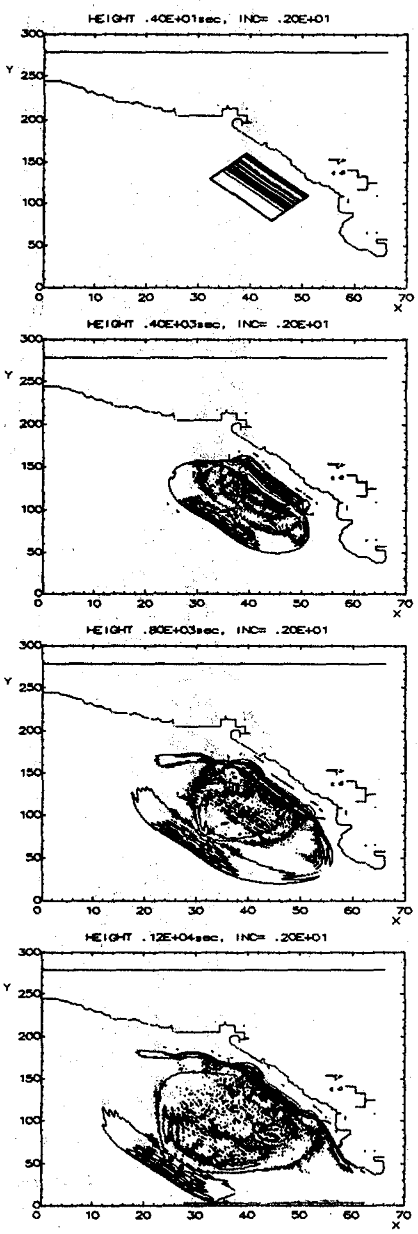

Figure 2. The 1992 Nicaragua tsunami wave propagation from the earthquake source. The contour interval is 2.0 meter.

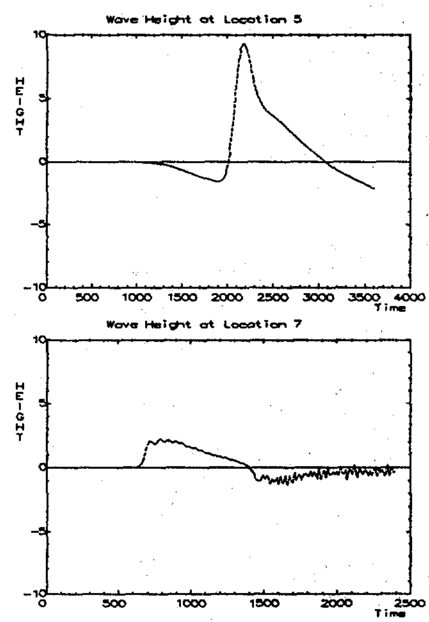

Figure 3. The Nicaragua earthquake source tsunami wave at two locations. Location 5 is 70 kilometers East of the earthquake epicenter near the shore and on the shallow shelf in 11 meters of water. Location 7 is in 3700 meters of water 220 km West of earthquake epicenter.

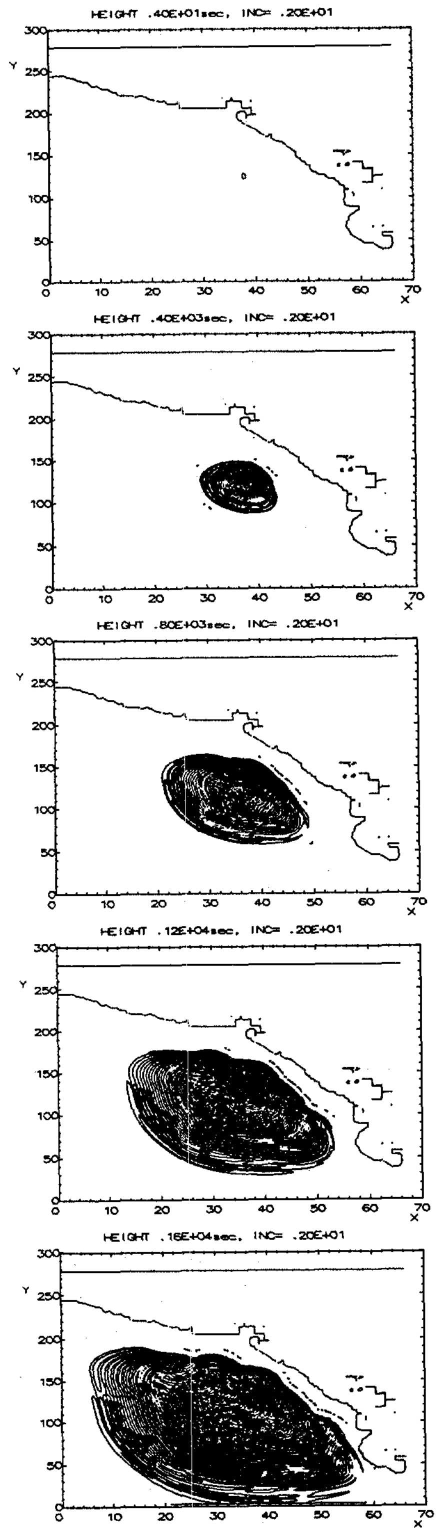

Figure 4. The Nicaragua tsunami wave propagation from the landslide source. The contour interval is 2.0 meter.

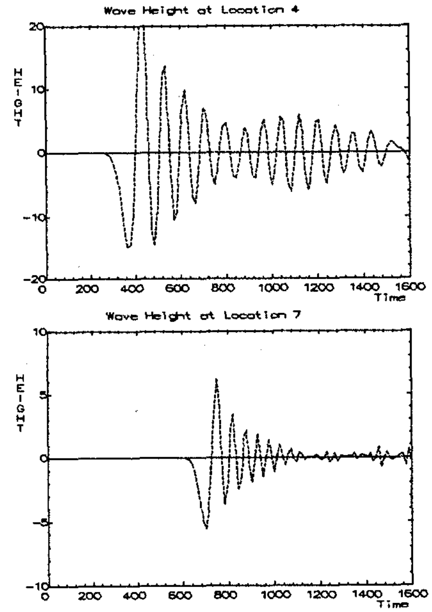

Figure 5. The landslide source Nicaragua tsunami wave at two locations. Location 7 is in 3700 meters of water 140 km West of the landslide. The height scale is 10 meters. Location 4 is 50 kilometers East of the landslide toward the shore in 450 meters of water. The height scale is 20 meters and the mesh size is marginal for such short period waves at this depth.

THREE DEADLY TSUNAMIS IN ONE YEAR

Augustine S. Furumoto
Hawaii Institute of Geophysics
School of Ocean and Earth Sciences and Technology
University of Hawaii at Manoa, Honolulu, Hawaii, U. S. A.

Abstract

Within an interval of one year, three destructive and deadly tsunamis claimed thousands of lives, namely the Nicaragua earthquake and tsunami on September 2, 1992, the Flores Island (Indonesia) earthquake and tsunami on December 12, 1992, and the Hokkaido Southwest (Japan) earthquake and tsunami on July 12, 1993. The Nicaragua tsunami did not conform to the common notion of a powerful bore or of a huge charging wave; instead it manifested itself as a gradual rise in sea level. The Flores Island and Hokkaido tsunamis were generated by back arc thrust fault earthquakes. All three events came under the class of tsunami earthquakes, where the accompanying tsunami is much larger than that expected from generating source revealed by seismological data. The three cases showed that even moment magnitude can be unreliable for estimating tsunami size.

Introduction

During 1992 - 1993 within an interval of one year, three devastating tsunamis claimed thousands of lives. The Nicaragua tsunami of September 2, 1992 drowned 170 people, injured 500 more and left 15,000 people homeless (Global Volcanic Network, 1993); the December 12, 1992, Flores Island, Indonesia, tsunami killed 2080 persons and left tens of thousands more homeless (Yeh et al., 1993); and the Hokkaido Southwest, Japan, earthquake and tsunami on July 12, 1993 claimed 330 lives and wiped out a major portion of the town of Aonae in Okushiri Island (Shukan Asahi, 1993). An examination of tsunami history showed that previous to 1992 there is no record of three such deadly tsunamis in the time span of twelve months. Besides the proximity to one another in time, these tsunamis had unusual characteristics, which warrant a descriptive article about them.

The Nicaragua Earthquake and Tsunami.

Much of the information and data concerning this earthquake and tsunami were collected by an international post-tsunami survey team, in which Japanese scientists formed the core and Kuniaki Abe was the team leader.

On September 1, 1992 at 6.16 PM Nicaragua time (September 2, 00h 16m 00s GMT), a Ms 7.2 earthquake was barely felt by residents along the coast of Nicaragua. The earthquake intensity was II on the Modified Mercalli Scale, and only at three places -- El Transito, La Boquito and San Juan del Sur -- was the intensity III. Only those who were sitting or standing very still could have felt the earthquake. Most people who felt the vibrations ignored them. In 40 to 70 minutes after the earthquake, the sea began to rise gradually, to 4 meters above the ambient sea level in most places along a 200 km stretch of the coast, higher in several places. Because the tsunami was a gradual rise of sea level rather than a bore or a crashing huge wave, most of the people were able to escape to dry ground. Those who perished were children under five years of age and the elderly who were unable to wade to safety through the rising water. In those villages where people died in the tsunami, the tsunami wave height was over 4 m. The highest wave height measured by the international tsunami survey team was at El Transito where the third wave was estimated to have reached 10.7 m (Kuniaki Abe et al., 1993).

The epicenter of the earthquake was 11.81° N, 87.35° W, right in the area designated as a seismic gap by Harlow et al. (1981). The seismic moment was 3×10^{20} Nm, which is equivalent to a moment magnitude of Mw = 7.6. By aftershock distribution, the rupture area of the earthquake was 250 km by 100 km (Kuniaki Abe, 1992). The tsunami source region coincided with the rupture area, as the 4 m run up extended for 200 km along the Nicaraguan coast (Figure 1).

The discrepancy of surface wave magnitude Ms = 7.2 and moment magnitude Mw = 7.6 led Kuniaki Abe et al. (1993) and Satake et al. (1993) to conclude that this was a "tsunami earthquake" as defined by Kanamori (1972) and further described by Pelayo and Wiens (1992). The earthquake source mechanism consisted of three subevents, each event being a reversed faulting along a plane dipping eastward at 16° (Ide et al., 1993).

For this event the Pacific Tsunami Warning Center did not issue a tsunami alert. The judgment was based (1) on the sea level recordings that came in from Ecuador, Galapagos Islands and other islands off the Central American Coast and (2) on the directivity of the tsunami. None of the tide gages registered a rise in sea level over 1 m. The main energy of the tsunami in the far field passed to the south of New Zealand and headed for the Antarctic region (Blackford, 1993). In hind sight this was a correct decision, as the tsunami amplitudes in the far field were all under 1 m.

Flores Island, Indonesia, Earthquake and Tsunami.

Of the three events we are discussing, the Flores island earthquake and tsunami of December 12, 1992 was the most disastrous. Of the 2080 persons who died, half were claimed by the tsunami. Tens of thousands were left homeless. A post tsunami international survey team was organized, again with Japanese scientists as the core, but this time the team leader was Yoshinobu Tsuji (Tsuji et al., 1993; Yeh et al., 1993).

Earthquake source parameters determined by the U. S. National Earthquake Information Center are: origin time of earthquake, 1992 December 12, 05h 29m 27s (GMT); epicenter 8.3° S, 122.3° E, normal depth at 33 km; surface wave magnitude Ms = 7.5; seismic moment Mo = 6.4×10^{20} Nm, which is equivalent to moment magnitude of Mw = 7.8. The fault motion was a thrust motion along a fault dipping 32° to the south. Yeh et al. (1993) computed the slip to be 3.2 m. The earthquake occurred in the Flores Sea, a marginal sea on the continent side of the island arc system known geographically as the Lesser Sunda Islands (Figure 2). The dimensions of the rupture area as determined by aftershocks are 110 km by 30 km (Tsuji et al., 1993).

The tsunami generated by the earthquake rushed into the shores of Flores Island and offshore lesser islands 3 to 4 minutes after the earthquake. Many villages were destroyed entirely; it is surprising that there were any survivors from these villages. On Babi Island within the rupture area of the earthquake, tsunamis approached the 2 km diameter island from three separate directions and swept away all buildings so that the island seemed as though it was returned to its virgin natural state with gleaming white sandy shores where once densely clustered houses stood. According to one report, of the 1093 inhabitants of the island, 800 survived and nearly 300 perished (Tsuji et al.,1993). Three days after the tsunami, the Indonesian government had to relocate all survivors from Babi Island to Flores Island as the tsunami had destroyed means of livelihood in Babi Island (A television report by NHK of Japan).

In Figure 3 are shown run ups as measured and compiled by the post tsunami survey team (Yeh et al. 1993). The rupture area from aftershocks has also been drawn in to show the proximity of the tsunami source area to points where tsunami run ups were measured. From the run ups it can be inferred that the vertical component of the earthquake slip must be in the order of 10 m.

The Flores Island earthquake occurred on the continent side of the island arc called the Lesser Sunda Islands. Because of its location with respect to tectonic features, this is considered to be a back arc thrust fault earthquake. A discussion of back arc tectonic earthquakes is given later in this article.

Hokkaido Southwest Earthquake and Tsunami.

On the night of July 12, 1993, at 10.17 PM, Japan Standard Time, an earthquake of magnitude Ms = 7.8 rocked the western shores of the island of Hokkaido and the neighboring lesser islands (Figure 4). The vibrations were severe enough to cause landslides, one of which buried a hotel in Okushiri Town on Okushiri Island and killed 30 people. Five minutes later a tsunami invaded Okushiri Island claiming over a hundred lives; then it hit Hokkaido proper claiming more lives (Figure 5). The Fifth Ward of Aonae Town on the southern tip of Okushiri Island was swept clean by two waves from the tsunami. The first wave with a height of 10 m came in from the west five minutes after the earthquake; the second wave with height over 5 m came in several minutes after the first wave from the opposite direction, the northeast (Figure 6). One out of three residents of the Fifth District, about 70 people, perished in the tsunami. The death toll would have been higher, had it not been for the alertness of the residents. As soon as the shaking of the earthquake died down, the residents began running for high ground with only their clothes, leaving everything else behind (NHK a, 1993).

As if death and destruction by tsunami were not enough, the earthquake itself had started fires in residential districts on high ground. Fire engines were blocked from going to the burning areas by debris thrown up by the tsunami. The unlucky homeowners had to watch their houses go up in flames despondently (NHK a, 1993).

By coincidence a television camera crew from Channel NHK, the Japanese public television system, happened to be staying in Aonae town that night to produce a documentary about fishermen. The crew fled with the people after the earthquake and filmed the incidents that were mentioned in the two paragraphs above.

The source parameters of the earthquake were: origin time 1993 July 12, 13h 17m (GMT), epicenter 42.8° N, 139.2° E, surface wave magnitude Ms = 7.8, depth 34 km, seismic moment 4.2×10^{20} Nm, moment magnitude Mw = 7.7. The rupture mechanism was reverse faulting with compression in the east-west direction along a plane dipping 30° to the east. The average slip as determined by seismological data was 3.5 m and the stress drop was 60 bars. The rupture area outlined by aftershocks included Okushiri Island; its dimensions were 100 km by 40 km with the long axis in the north-south direction (Japan Meteorological Agency, 1993).

As Okushiri Island had suffered damages in 1983 from the Japan Sea Chuubu tsunami, in the late 1980's a seawall 4.5 m high had been constructed completely around the Fifth Ward of Aonae town to protect the ward from future tsunamis. In spite of that precaution, the tsunami of 1993 with a wave height of 10 m topped the sea wall and demolished the Fifth Ward.

Government response to the disaster was swift. Homeless survivors from the tsunami and fires were housed in school gymnasiums that night and the next few nights. The very next morning injured persons and persons rescued from the sea by fishing boats were flown to Hakodate City in Hokkaido for medical treatment. In a matter of less than a week, temporary cottages were constructed on high ground and the survivors of the fire and tsunami were housed in them. These cottages, pre-designed, pre-fabricated and available for emergency housing following disasters, have the necessary amenities for living: water, electric power and sewer connections. In a week the survivors were gallantly going back to normal life: fishermen cleaned the debris and went back to fishing, and school children returned to school, although they all carried the emotional scars of that harrowing night (NHK b, 1993).

There are two factors that deserve our attention. The alertness of residents in coastal areas kept down the death toll. Government action in mitigation planning and swift response hastened recovery to a matter of weeks.

Back Arc Thrust Fault Earthquakes.

The Flores Island and Hokkaido Southwest earthquakes were back arc thrust fault earthquakes as described by Plafcker and Ward, (1992). This type of earthquakes belong to the class of subduction earthquakes but occur less frequently than the conventional subduction earthquakes associated with oceanic trenches. In Figure 7 is shown the structure of an island arc system with back arc subduction. On the right of the island arc where the ocean -- it could be the Pacific Ocean or the Indian Ocean -- is located, the oceanic lithospheric plate burrows under the island arc because the oceanic plate is denser than the island arc, which is usually a fragment of an ancient continent. Earthquakes caused by the subduction of the oceanic plate under the island arc defines the Benioff-Wadati zone. Great earthquakes and giant tsunamis are generated in the subduction zone on the oceanic side. At a depth where the temperature is in the neighborhood 900° C, parts of the subducted oceanic plate melt to form magma pockets. Some of the magma finds its way to the surface to form andesitic and dacitic volcanoes.

On the continent side of the island arc system is a marginal sea, which is sometimes referred to as the back arc basin. The Sea of Japan is a textbook example of a back arc basin. The crust beneath the marginal sea also subducts under the island arc, from the back side, because the marine crust is denser than island arc crust. Unlike the oceanic side where seismologists have been able to delineate the Benioff-Wadati zone, geologists still do not have a clear idea of the boundary between the subducting marginal sea crust and island arc, simply because earthquakes in the back arc have not been numerous as on the ocean side.

However within the last few decades, back arc earthquakes have occurred more frequently than in previous decades and have drawn the attention of seismologists because of the destructive tsunamis accompanying these earthquakes. In addition to the Flores Island earthquake, recent examples of back arc earthquakes were the Niigata earthquake of 1964, the Sea of Japan Chuubu earthquake of 1983, the Costa Rica earthquake of April 1991 and the Hokkaido Southwest earthquake of 1993.

With the occurrence of the Hokkaido Southwest earthquake, we can now delineate the back arc subduction zone to the west of northern Japan (Figure 4). The Hokkaido Southwest earthquake has filled in the gap between the 1940 earthquake and 1983 Sea of Japan Chuubu earthquake. We speculate that the back arc subduction zone has been rather thoroughly ruptured and we can expect a more or less quiet period until the next series of rupturing earthquakes appear, perhaps for the next 200 years. As for the subduction zones on the Pacific ocean side of Japan, there appear to be some gaps that need to be filled.

Tsunami Earthquakes.

All three earthquakes described above fall into the class of tsunami earthquakes because the tsunamis were much larger than expected from the surface wave magnitudes and even from the moment magnitudes. In Table 1 are listed the source parameters of the earthquakes and tsunami run up data.

TABLE 1.
SOURCE PARAMETERS AND TSUNAMI RUN UPS

EVENT	MOMENT MAGNITUDE	SLIP (m)	VERTICAL COMP OF SLIP (m)	TSUNAMI RUN UP (m)	SEA BED UPLIFT (m)
Nicaragua	7.6	0.4	0.1	> 4	> 8
Flores Island	7.8	3.2	1.6	> 4	> 8
Hokkaido Southwest	7.7	3.5	1.8	> 5	> 10

Most of the source parameter data in the table have been given earlier in this article. The slip of the Nicaragua earthquake was calculated using the formula:

$$M_o = \mu A d$$

where μ is the modulus of rigidity of the rupturing material, A is rupture area and d is the slip. The value of the modulus of rigidity has been given by Yeh et al. (1993) as 4×10^{10} N-m. The vertical components of slip were calculated using dip angles given among the source parameter solutions. The tsunami run up values are the minimum value along the coast closest to the source. As the amplitude of a travelling tsunami in the near field is half the wave height of the initial tsunami, the sea bed must rise twice the value of the amplitude of the near field travelling tsunami.

From the table it can be concluded that in each case the sea bed rise required to generate the observed tsunami is larger by a factor of five than the vertical component of slip derived by seismological calculations. This has grave implications for tsunami numerical modelling studies and for tsunami warning.

In tsunami modelling the most critical parameter is the uplift of the seabed. If this parameter is not accurately determinable from seismological data, the forward problem is an empty exercise. On the other hand the inverse problem of determining tsunami source from tsunami data is valid. Tsunami data inversion may be the only certain method of deriving tsunami source.

For tsunami warning the uncertainty of seismological source parameters for ascertaining tsunami source is a very serious problem. The difficulty with surface wave magnitude has been well known among those engaged in tsunami warning. Now that even moment magnitude is questionable, precious few parameters are left to estimate tsunami size. A suggested solution to the impasse is the development of a rapid method for inverting near field tide gage data in real time to obtain tsunami source, then from the source to give quantitative forecasts to coastline communities in the far field.

Concluding Remarks.

The occurrence of three destructive and deadly tsunamis within one year was a rare phenomenon. The Nicaragua tsunami was a case where the tsunami manifested itself as a gradual rise in sea level. Able bodied persons were able to reach safety but the very young, the infirm and the aged were victims.

The Flores Island and Hokkaido Southwest earthquakes were back arc thrust faulting types. There has been an increase in the number of back arc earthquakes in the last few decades. The Hokkaido Southwest earthquake enabled seismologists to outline the back arc subduction zone west of northern Japan.

The swift government reaction to the Hokkaido Southwest earthquake and tsunami demonstrated the value of mitigation planning in returning to normalcy.

These tsunami earthquakes cast doubt on the reliability of estimating tsunami size from moment magnitude.

This is SOEST contribution no. 3486.

REFERENCES

Abe, Kuniaki, 1992. Rapid Survey Report on the 1992 September 2 Nicaragua Earthquake and Tsunami (in Japanese). News Letter, Seism. Soc. Japan, Vol. 4, no. 4, 3-7.

Abe, Kuniaki, Katsuyuki Abe, Y. Tsuji, F. Imamura, H. Katao, Y. Ito, K. Satake, J. Bourgeois, Evelyun Noguera and F. Estrada. 1993. Field survey of the Nicaragua earthquake and tsunami of September 2, 1992. Bull. Earthquake Res. Inst, vol. 68, 23-70.

Asahi Shukan, 1993. Okushiri Island doomed. (in Japanese). Asahi Shukan, issue of July 30.

Blackford, M., 1993. Statement made at a workshop at State Civil Defense, Honolulu, Hawaii.

Global Volcanism Network, 1993. Geologic Phenomena. Geotimes, Vol. 38, no. 1, 21.

Harlow, D. H., R. A. White, I. L. Cifuentes and A. Aburto, 1981. Quiet zone within a seismic gap near western Nicaragua: Possible location of a future large earthquake. Science, vol. 213, 648.

Hokkaido Tsunami Survey Group, 1993. Tsunami devastates Japanese coastal region. EOS, vol.74, no. 37, 417-432.

Ide, S., H. Imamura, Y. Yoshida and Katsumasa Abe, 1993. Source mechanism of the Nicaraguan tsunami earthquake of September 2, 1992. Proc. IUGG/IOC Int. Tsunami Symposium, Wakayama, Japan. 637-646.

Japan Meteorological Agency, 1993. Southwest Hokkaido Earthquake. Rapid Bulletin on Disasters, August 1, 1993 issue.

Kanamori, H., 1972. Mechanism of tsunami earthquakes. Phys. Earth Planet. Inter. vol. 6, 346-359.

NHK, 1993 a. The Tsunami Invasion. (A television documentary).

NHK, 1993 b. One month after the earthquake. (A television documentary.)

Pelayo, A. M., and D. A. Wiens, 1992. Mechanism of tsunami earthquakes: Slow thrust-faulting events in the accretionary wedge. Jour. Geophys. Res. vol. 97, 15,321 - 15,337.

Plafker, G., and S. N. Ward, 1992. Backarc thrust faulting and tectonic uplift along the Caribbean sea coast during the April 22, 1991 Costa Rica earthquake. Tectonics, vol. 11, 709-718.

Satake, K., J. Bourgeois, Kuniaki Abe, Katsuyuki Abe, Y. Tsuji, F. Imamura, Y. Iio, H. Katao, E. Noguera and F. Estrada, 1993. Tsunami Field Survey of the 1992 Nicaragua Earthquake. EOS vol. 74, No. 13, 145-158.

Tsuji, Y., F. Imamura, H. Matsutomi, K. Kawada, J. Shibuya, M. Kashino, M. Takeo, M. Matsuyama, and T. Takahashi. 1993. Rapid Report of 1992 December 12 Indonesia Flores Island earthquake and tsunami (in Japanese). News Letter, Seism. Soc. Japan, vol. 4, no. 6, 4-8.

Yeh, H., F. Imamura, C. Synolakis, Y. Tsuji, P. Liu and S. Shi, 1993. The Flores Island Tsunamis. EOS vol. 74, no. 33 369-373.

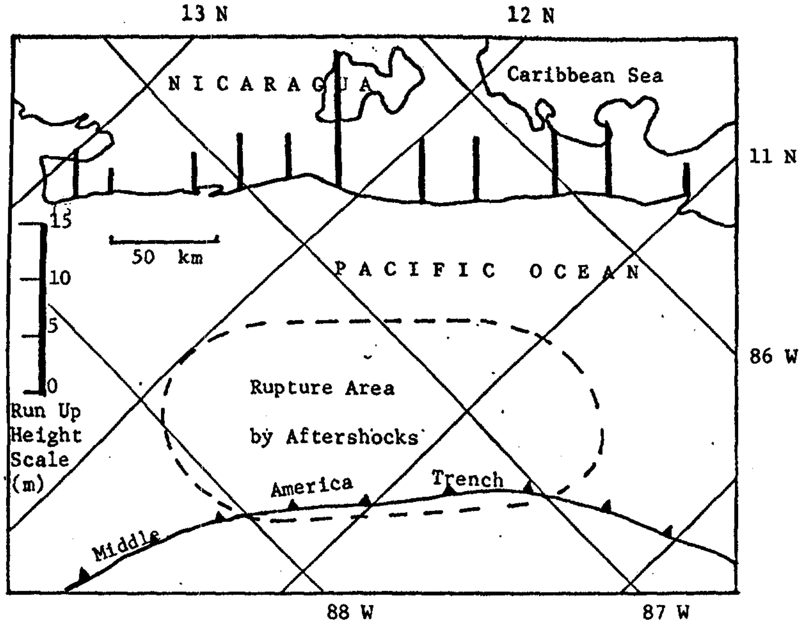

Figure 1. Rupture Area and Tsunami Run Up Heights along the Nicaraguan Coast for Earthquake and Tsunami of September 2, 1993. Data from Satake et al., 1993.

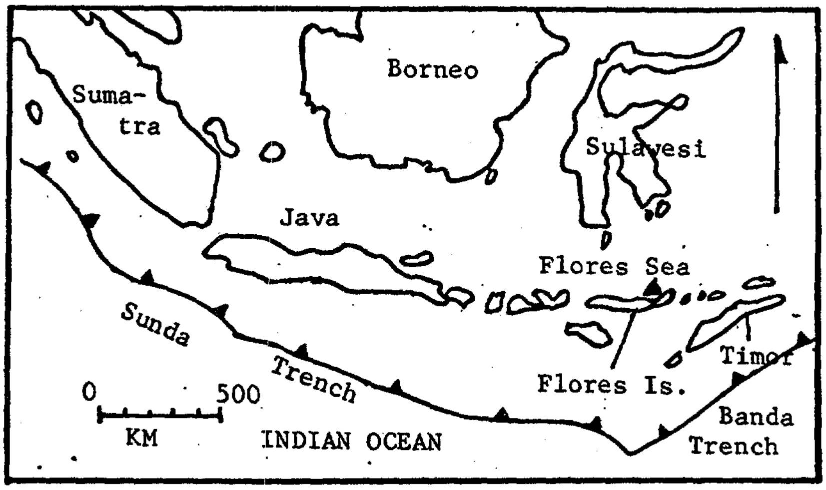

Figure 2. Epicenter (filled triangle) of Flores Island Earthquake. Redrawn from Yeh et al., 1993.

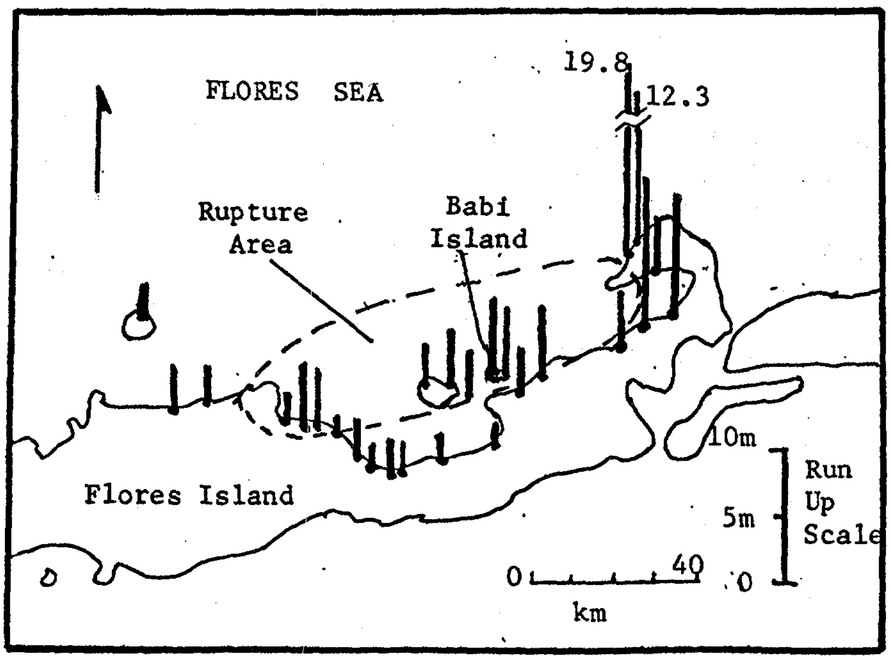

Figure 3. Rupture Area and Tsunami Run Up Heights of Flores Island Earthquake. Run up data from Yeh et al., 1993.

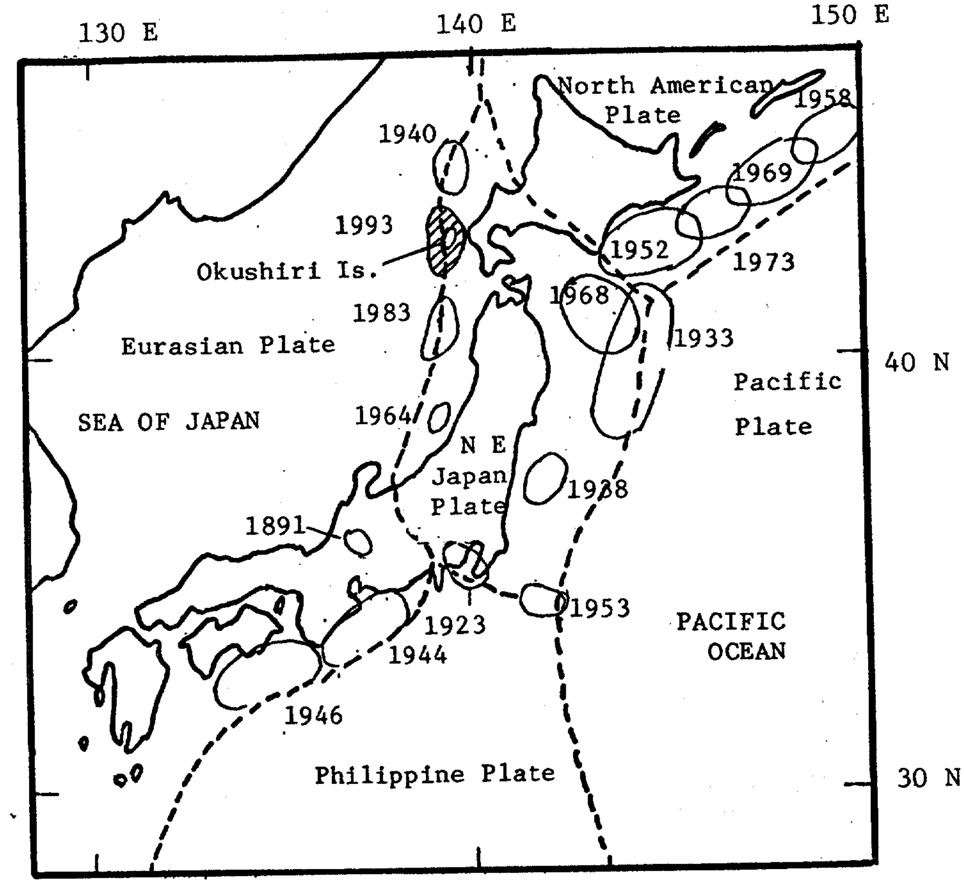

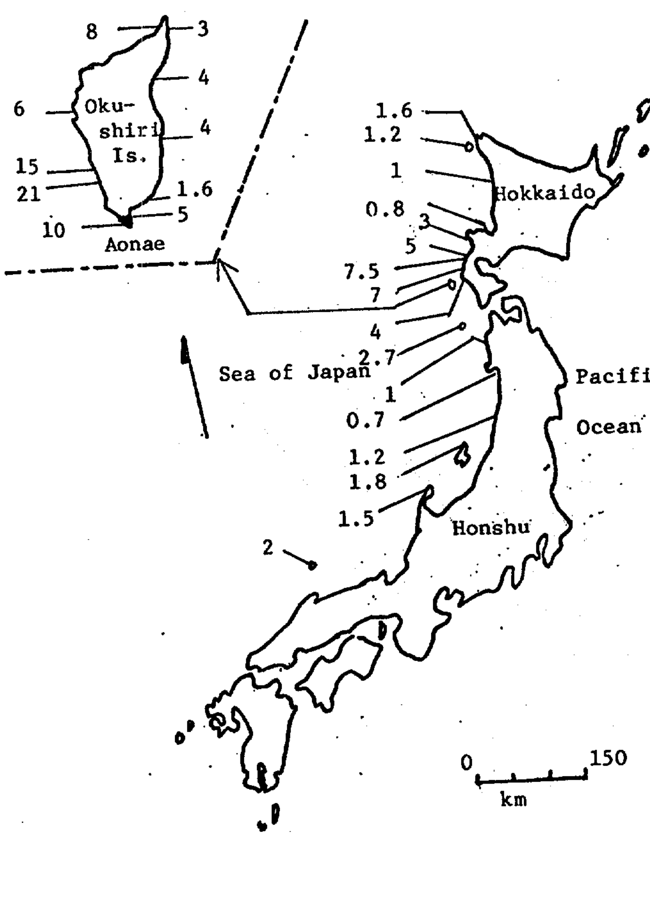

Figure 4 (above). Rupture area of the July 12, 1993 earthquake (shaded) and rupture areas of large earthquakes in the last 100 years. Broken lines are boundaries of lithospheric plates.

Figure 5. Tsunami run ups in meters from the July 12, 1993 earthquake. Data from Japan Meteorological Agency, 1993.

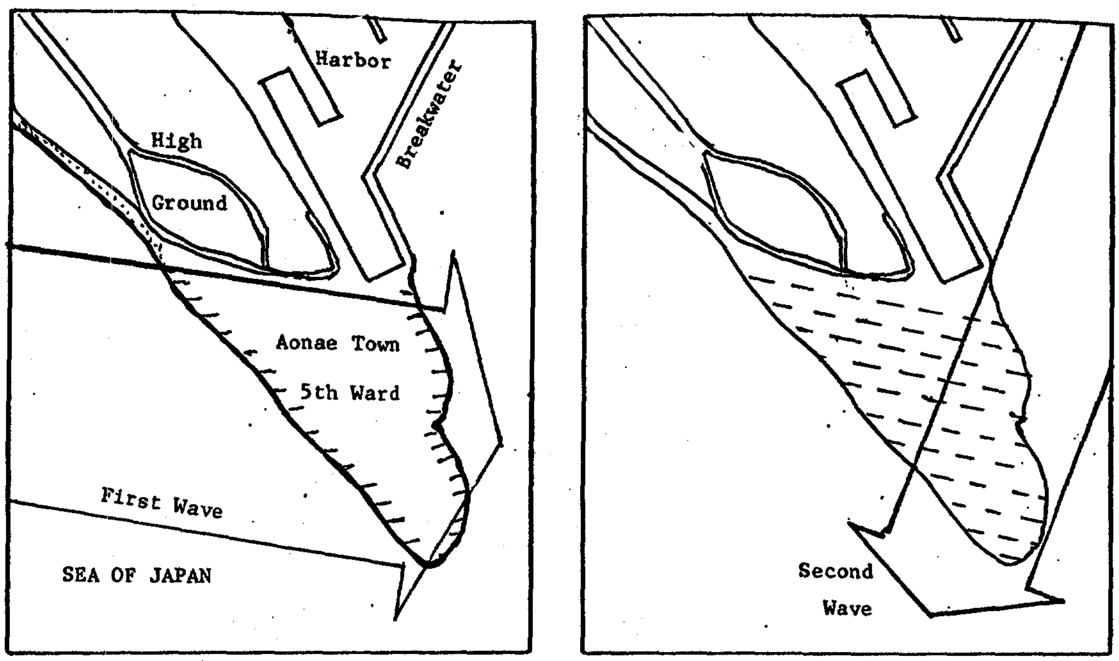

Figure 6. Two waves demolish Aonae Town Fifth Ward. The first came from the west and the second from northeast.

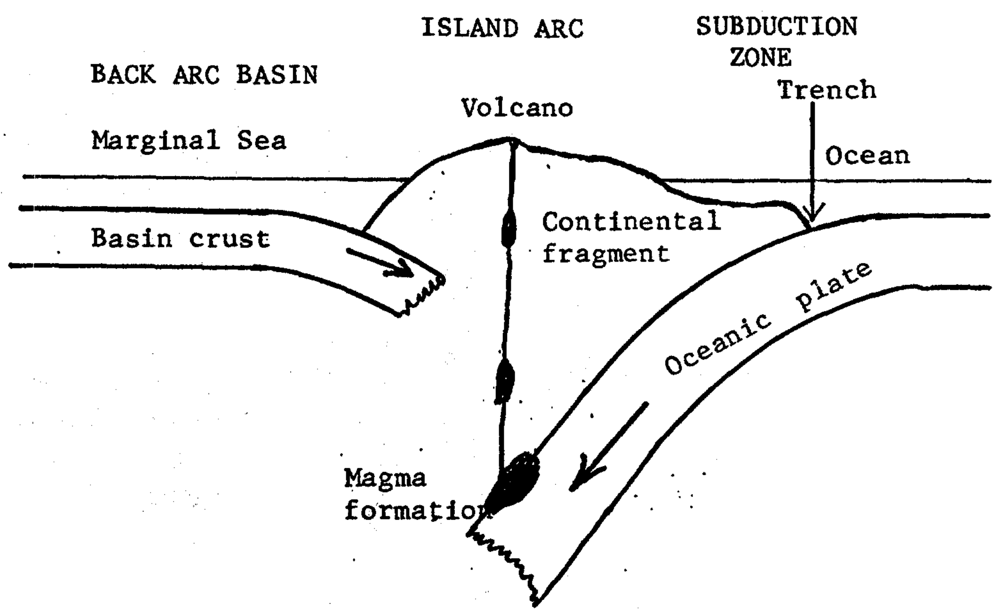

Figure 7. The arrangement of subduction zone, island arc and back arc basin.

SCENES OF DESTRUCTION

HOKKAIDO SOUTHWEST EARTHQUAKE AND TSUNAMI

JULY 12, 1993

Courtesy of International Tsunami Information Center,
National Oceanic and Atmospheric Administration,
Honolulu, Hawaii, U. S. A.

The following photographs were taken by Commander Dennis Sigrist, NOAA, member of post-tsunami survey team.

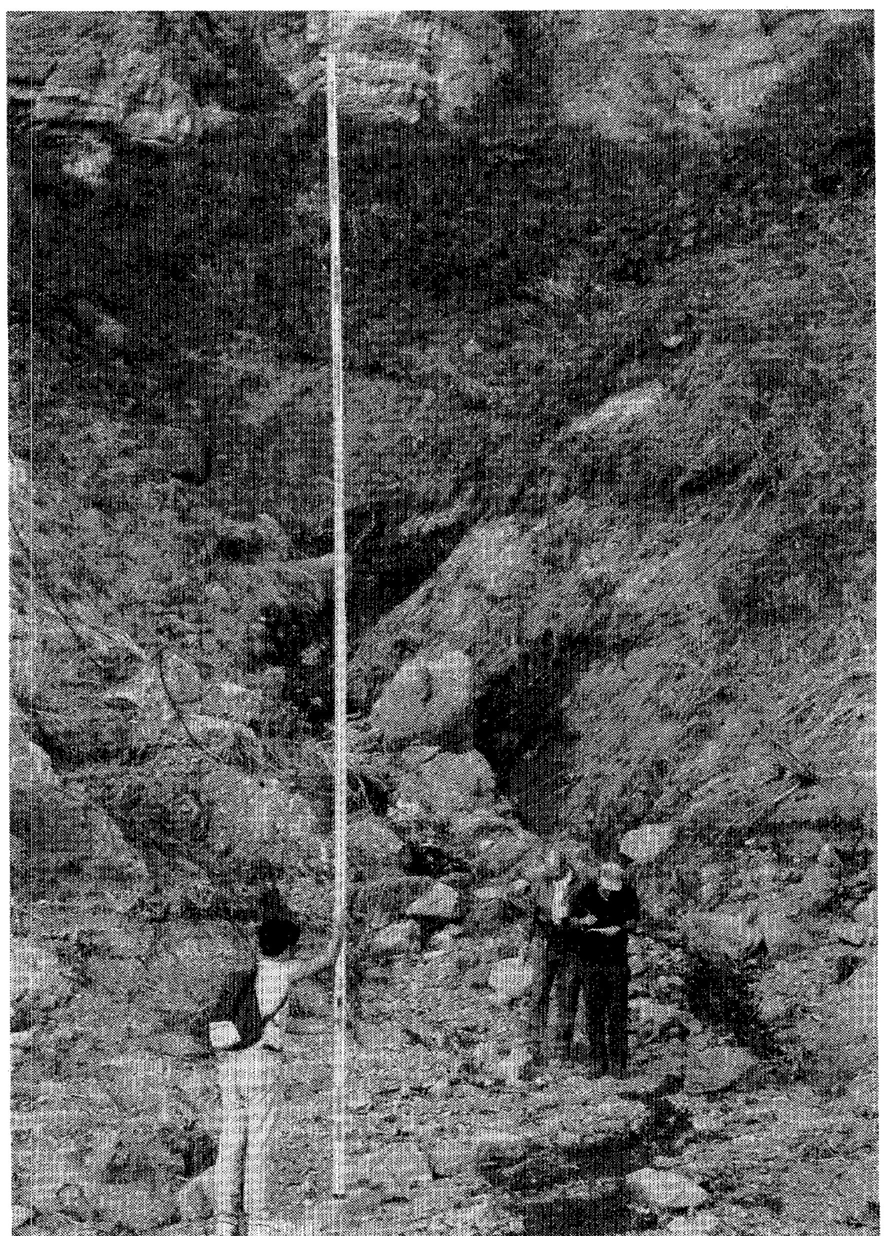

Gully near the village of Monai where the highest run up of 33 m was measured in post-tsunami survey.

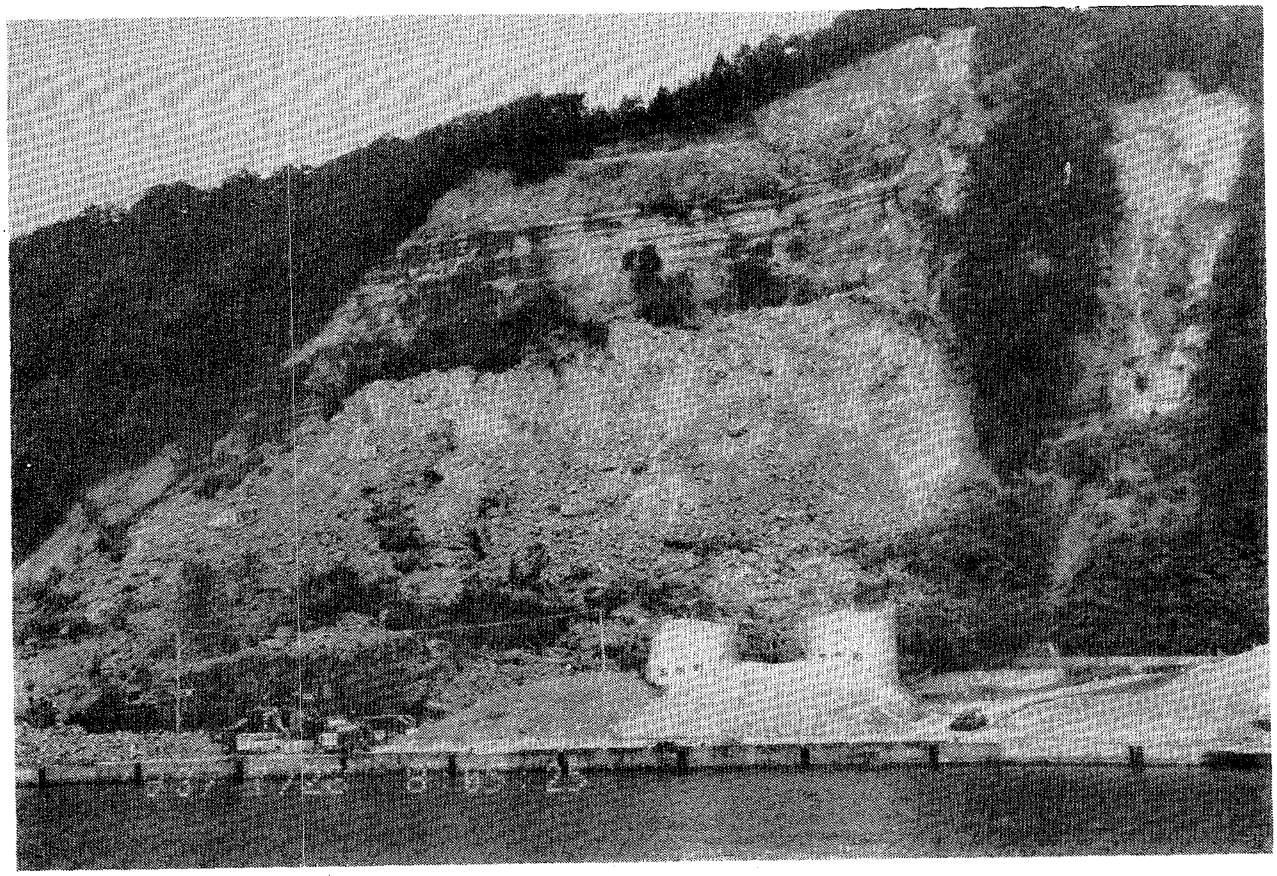

Landslide at Port Okushiri, Okushiri Island, which buried Yoyoso Hotel.

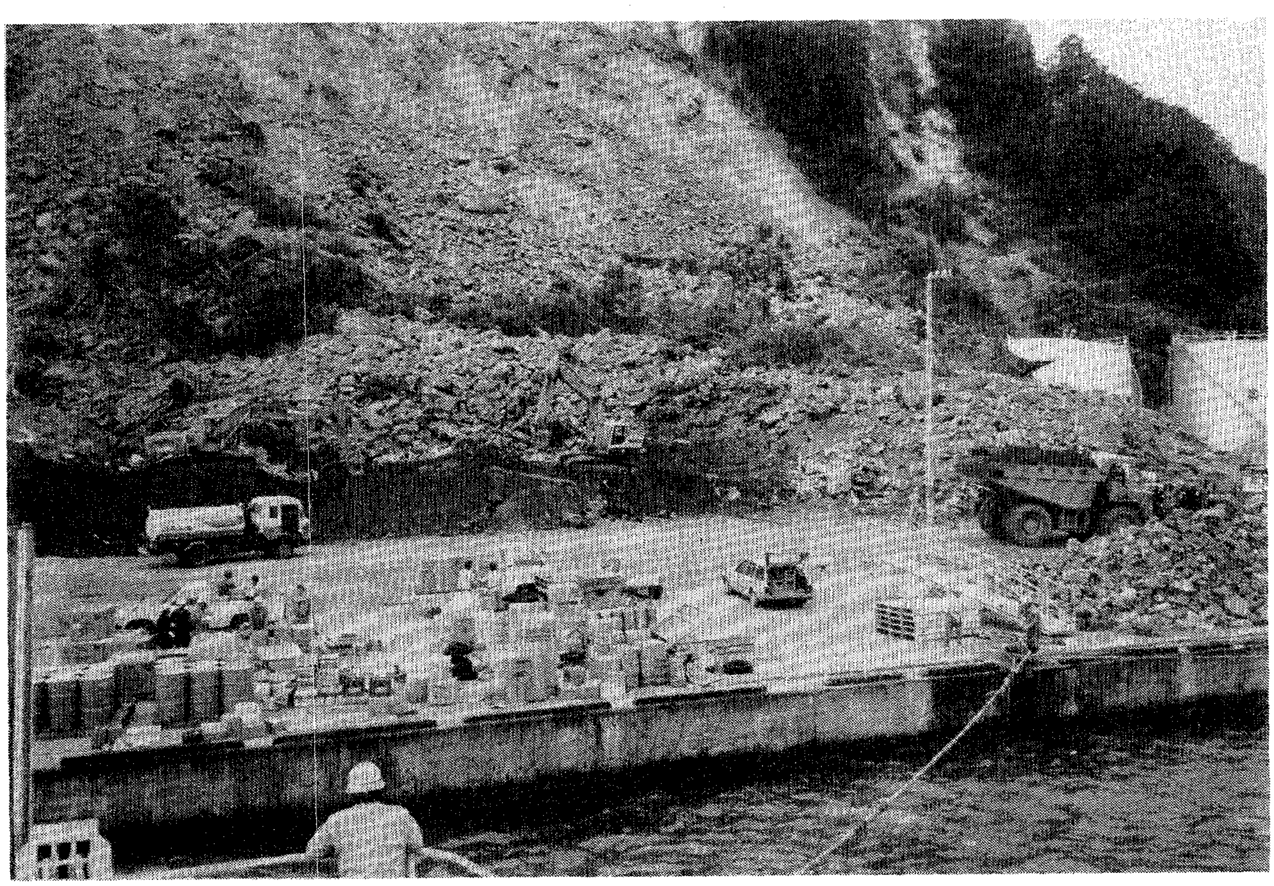

Closer view of landslide. The hotel was completely covered.

Aonae Harbor flattened by tsunami.

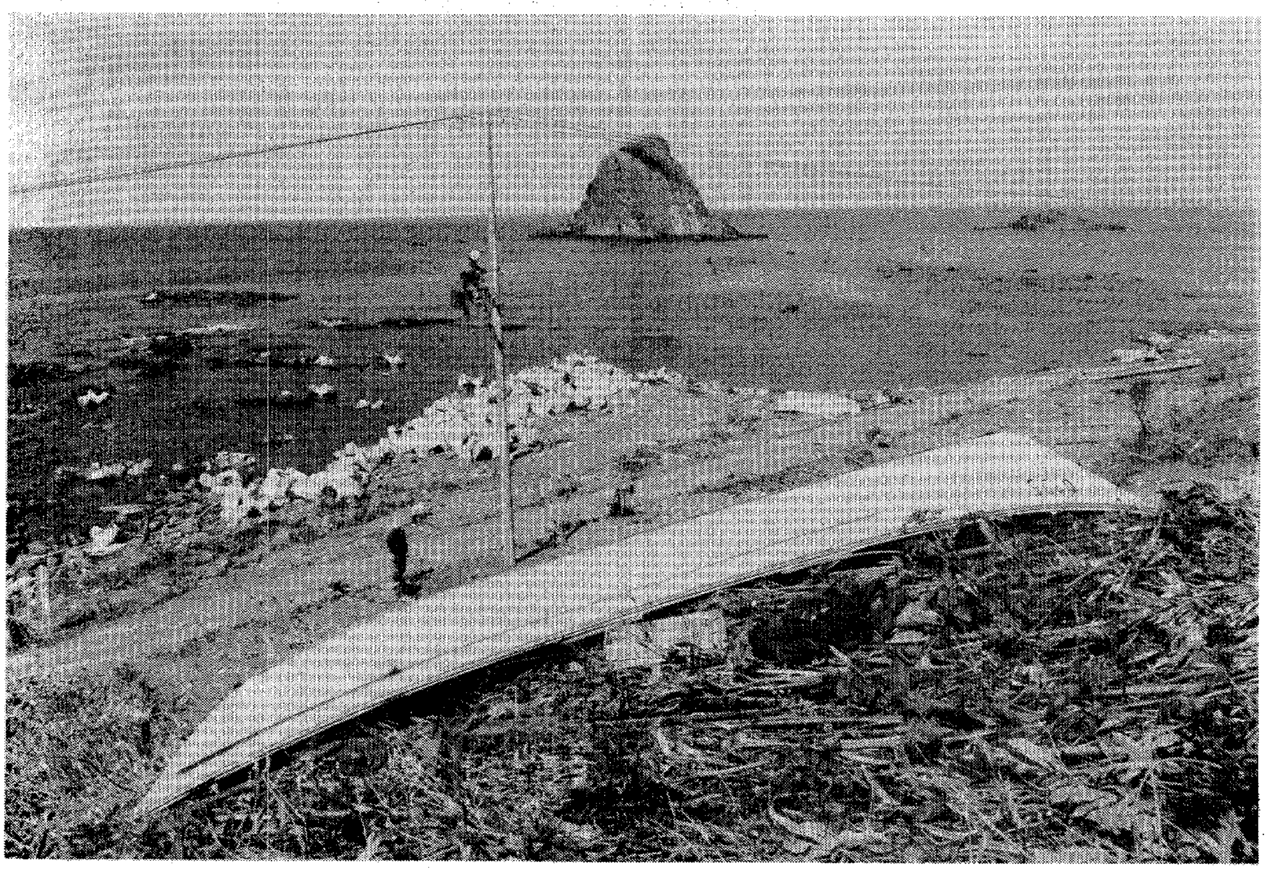

The tsunami had beached a skiff on a bluff over 10 m high.

The Tsunami Research Problem

George D. Curtis
Tsunami Research Specialist, Joint Institute for Marine and Atmospheric Research and Affiliate Professor, Marine Science, University of Hawaii--Hilo

This a note discussing past and current tsunami research, the results it has produced, and suggesting how it may be oriented in the future to better serve public safety needs.

The Reason

The primary reason for tsunami research is to save lives and, to a lesser extent, property (Curtis, 1991). With the development of a working warning system for the Pacific in 1948 this goal became achievable. The system has never missed a damaging tsunami, although initially the false alarm rate was a problem. With more sea level/tide gages, telemetry, better communications, and faster seismic analysis, the Pacific Tsunami Warning System is highly functional, although the lack of major events in the past two decades has not exercised it fully. Concern has become more focused on evacuation and on local tsunamis. A detailed table on hazard mitigation in the above reference emphasizes the public safety factors involved in tsunami efforts, and may be summarized as follows: Mitigation of tsunami hazards involves people and structures. For structures, zoning and codes handle the problem routinely. But for people, a highly reliable warning system, prepared zones and plans for evacuation, and education of both the public and officials is essential. A number of tasks are listed to accomplish or improve these factors. The tasks outlined will be examined further, covering <u>prediction</u> (initial warning), <u>propagation</u> (evaluation of the threat), and <u>terminal effects</u> (runup and wave forces).

Research -- Past and in Progress

Bernard and Goulet (1981) presented the expenditures, status, and recommended priorities for tsunami research at that time in several tables. These may be summarized as follows: In FY 1980, over $1,300,000 was spent on tsunami research; the largest amount was on propagation, followed by generation. NSF expended the most funds, followed by NOAA. The top priority recommendation was for instrument observations, with modeling of terminal effects next, followed by tsunamigenic earthquake identification. Since 1981, U.S. funding may have declined but significant Japanese and (former) Soviet funds have been expended. It is probably not a coincidence that there have been no major U.S. or Pacific-wide tsunamis since 1964; unfortunately, disaster begats funds. However, the combined research efforts in the past decade or so have involved and produced a large body of studies and some results concerning the following:

- telemetry of tide stations and research-oriented sea level gages to the Warning Center has greatly aided evaluation of a possible tsunami.
- establishment of the Alaska regional warning system, based on rapid response to seismic data has aided the hazard reduction from near and mid-range tsunamis. The Japanese have a similar system in place, and a local automatic version is in place in Chile (THRUST).
  (note that the above are operational improvements and not the result of specific research).
- more powerful computers and better programs have provided more rapid evaluation of tsunamigenic seismic events at the warning centers.
- a local monitoring/observational program was developed and put in place (Curtis, 1982).
- a one-dimensional method (developed for other purposes) was applied to the runup problem; using available historical information flood insurance maps were produced which involved tsunami effects. (Houston, et al, 1977)
- with additional data and procedures, the model was used to develop updated evacuation maps for the Hawaiian Islands. (Curtis, 1991).

- two-dimensional numerical models were developed and applied to the ocean propagation and to the runup problem (Mader, 1988; Kowalik and Whitmore, 1991).
- one of the 2-D models was applied from start-to-finish to actual Pacific-wide tsunamis, and tested against historical inundation records for Hilo (Mader et al., 1992).
- several deep ocean-bottom recording pressure sensors were deployed for a year or more and recovered for satisfactory analysis (Gonzalez, et al, 1989).
- numerous model studies were made of actual and possible nearby tsunami events, with extremely varied results when compared with observations. Little has been published other than the theoretical analyses.
- means to rapidly estimate the moment (and mantle) magnitude to aid in evaluation of possible tsunami generation by a seismic event were developed (Talandier and Okal, 1989).
- interest resumed in use of the acoustic T-phase, based on extensive analysis of a large data set from the Wake Island MILS hydrophones (Walker, 1993).

Thus, progress appears to have been considerable regarding the needs set forth in 1981. Yet, the requests for more support and the need for valid work continues. Why should this be so, and what research and applications are really necessary to reach all the goals of the 1981 report? How does this match the research priorities set ? If funding were continued at the 1980 rate, has the $25+ million spent since then brought us to expected goals? Where should available research dollars and skills be directed?

Unmet Research Needs

Based on publications, seminars, and the numerous conferences and/or sessions on tsunamis, the following seems to be the situation:

- a great amount of effort has been expended, both in field work and in numerical modeling, on local tsunamis (Nicaragua, Indonesia, etc) with little useful output. The models have not proven to be good predictors of runup, partly due to lack of knowledge of the seismic action and partly due to the limitations of the models in shallow water and the near field. There seems to be little reason for major efforts to overcome these problems, since there is little use for the resulting data even if it were valid. Furumoto (1993) has vividly described the recent tsunamis in Indonesia, Nicaragua and Japan, and related them to the modeling and warning problems. Unless there is a reasonable warning time and a fast-response warning system in place, detailed analyses of the wave action from such events are futile with regard to the public safety goal and would better be applied to other problems. - the near field problem, before a fully developed wave is formed, is a major discrepancy in modeling and must be better resolved and tested against reality in the mid- and long-range. Likewise, coupling into the ocean is as imperfectly understood as is ground motion. The rather deep 8.1 earthquake near Guam, which resulted in a short-lived warning, but no tsunami, is an example which could be studied to improve both evaluation for warning and ocean model inputs.
- reducing the "false alarm" rate of the warning systems--without impairing their reliability--is certainly the most cost effective achievement which may be feasible. The 1986 warning was estimated to cost as much as $30 million in Hawaii alone. Better rapid evaluation of the source and initial propagation is needed; areas involved seem to be as follows:

  Source- a) seismic evaluation: we should continue the work with long-period and acoustic data, with the addition of any new schemes and investigators showing promise. b) it is time to utilize modern equipment and capability to further develop evaluation methods which have received brief trials in the past but should have the ability to reveal vertical displacement of the ocean surface. Two of these are infrasonic and ionospheric detection.

  Initial propagation- in the time period after the waves develop but while there is still warning time, a final evaluation of their hazard is needed, and in the future can be made. The further development of the long-awaited ocean bottom pressure sensors, as demonstrated in PACTOPS, with surface transmitters added, will permit this. It will do so best if the data are fed directly to a prepared model such as presently available. As outlined previously (Curtis and Mader, 1987), such a model can already use some data that are now available to provide an improved, progressive prediction in real time.

- Terminal effects: since the primary goal is to save lives, evacuation of susceptible coastal areas upon a warning is vital. Definition of these areas was first accomplished by Cox (1961) and recently with more refined methods for the Hawaiian Islands by Curtis (1991). The one dimensional model used was supplemented in selected locations by a 2-D model of Mader, which has been tested against detailed historical data in the Hilo Bay area (Mader and Curtis, 1992). It was found that additional work is needed in the application of such modeling in evaluation of friction factors, feasible grid sizes, shallow water limitations, and comparisons with 1-D methods and with observed effects. One important use of valid ocean models may often be to input the near-shore wave heights produced, to more simple runup/inundation analytical procedures used to cover larger areas.
- Observation - Whether we are depending on historical data for our primary hazard levels or using it for testing of a model, it must be collected rapidly, on short notice, and accurately. We can neither test a model nor estimate inundation without such data. The cost of most coastal monitoring programs is not great. They should be implemented in all tsunami-prone areas for which evacuation zones are to be developed--and must be maintained for many years.

What Next ?

It is hoped the above observations will provoke interest and discussions by policymakers, funding agencies, and sincere researchers who are willing to give a priority to public benefit.
Money, and even skilled, responsible researchers are usually in short supply, and we must do our best to utilize them in the public interest.

References

Bernard, Eddie, and Richard Goulet, 1981. Tsunami Research Opportunities, NSF/NOAA, Washington DC.

Cox, Doak, 1961, "Potential Tsunami Inundation Areas in Hawaii", Hawaii Institute of Geophysics Report No. 14. University of Hawaii, Honolulu.

Curtis, George, 1991. "Hawaii Tsunami Inundation/Evacuation Map Project", published by the Joint Institute for Marine and Atmospheric Research, University of Hawaii.

Curtis, George and Charles L. Mader, 1987. "Real-time Monitoring and Modeling for Tsunami Threat Evaluation", Science of Tsunami Hazards, V5, N1.

Curtis, George, 1982, "Establishment and Operation of a Tsunami Monitoring Program", Science of Tsunami Hazards, V1, N1.

Furumoto, Augustine S., 1993, "Three Deadly Tsunamis in One Year", Science of Tsunami Hazards, V11, N2.

Gonzalez, F. I., E. N. Bernard, M. C. Eble, and Charles L. Mader, 1989, "The Recent Alaskan Tsunami: Deep Ocean Measurements and Model Results", Proc. International Tsunami Symposium, Novosibirsk.

Houston, J.R., R.D. Carver, and D.G. Markle, 1977. "Tsunami-wave Frequency for the Hawaiian Islands", Technical Report H-77-1, U.S.Army Engineers Waterways Experiment Station, Vicksburg, Miss.

Kowalik, Zigmunt, and Paul Whitmore, 1991, "An Investigation of Two Tsunamis Recorded at Adak, Alaska", Science of Tsunami Hazards, V9, N2.

Mader, Charles L., 1988. Numerical Modeling of Water Waves, University of California Press, Berkeley.

Mader, Charles L., and George D. Curtis, 1992. "Modeling Tsunami Flooding of Hilo Hawaii", in Recent Advances in Marine Science and Technology, PACON, Honolulu.

Talandier, J., and E. E. Okal, 1989, "An Algorithm for Automated Tsunami Warning in French Polynesia based on Mantle Magnitudes", Bull. Seismol. Soc. Am., 79-4.

Walker, Daniel A., 1993, "Pacific-Wide Tsunamis Reported in Hawaii from 1819 through 1990: Runups, Magnitudes, Moments, and Implications for Warning Systems", Technical Report to Pacific Tsunami Warning Center, University of Hawaii. (submitted for publication)

APPLICATION FOR MEMBERSHIP

THE TSUNAMI SOCIETY
P.O. Box 8523
Honolulu, Hawaii 96815, USA

I desire admission into the Tsunami Society as: (Check appropriate box.)

☐ Student ☐ Member ☐ Institutional Member

Name ______________________ Signature ______________________
Address ______________________ Phone No. ______________________
____
Zip Code ______________________ Country ______________________
Employed by ____
Address ____
Title of your position ____

FEE: Student $5.00 Member $25.00 Institution $100.00
Fee includes a subscription to the society journal: SCIENCE OF TSUNAMI HAZARDS.

Send dues for one year with application. Membership shall date from 1 January of the year in which the applicant joins. Membership of an applicant applying on or after October 1 will begin with 1 January of the succeeding calendar year and his first dues payment will be applied to that year.